

Assimilation of wave spectra from pitch-and-roll buoys in a North Sea wave model

A.C. Voorrips and V.K. Makin

Royal Netherlands Meteorological Institute, De Bilt, Netherlands

S. Hasselmann

Max-Planck-Institut für Meteorologie, Hamburg, Germany

Abstract.

A technique for the assimilation of spectral wave observations in wave models is presented and tested. The method uses the concept of spectral partitioning to project the entire wave spectrum onto a few essential mean parameters. Model and observed partition parameters are assimilated using an optimal interpolation (OI) technique. After data reduction, obtained by the partitioning, the cost of the assimilation is negligible compared to the cost of the model run itself. Therefore the optimal interpolation of partitions (OI-P) method is a very attractive assimilation technique for operational wave forecasting. The paper focuses on the assimilation of pitch-and-roll buoy spectra in a North Sea version of the WAM wave model. Treatment of the (non-fully two-dimensional) buoy spectra is discussed. Appropriate choices for the OI weight functions are made. The problem of correlating wave partitions in different spectra is addressed, which is essential for obtaining a robust and efficient system. In order to assess the influence of spectral wave observations on the analysis of the sea state, the method is compared to a second scheme, optimal interpolation of integral parameters (OI-I), which can only be used to assimilate observations of significant wave height and mean wave period. First, tests with synthetic data are described, which illustrate advantages of the partitioning method over the OI-I scheme. Also, the inherent limitations of OI are shown in both methods. Experiments with buoy observations for actual North Sea conditions show the benefits of the system, especially when several wave systems are present at the same time.

1. Introduction

Assimilation of wave observations in operational wave forecast models is a relatively new subject. For a long time, the lack of near-real-time available wave observations impeded the development of assimilation systems. With the advent of new observation systems, notably the altimeter and synthetic aperture radar (SAR) on board the European Remote Sensing satellites ERS 1 and ERS 2, this situation is beginning to change. It is now recognized that assimilation of wave observations can improve both the analyzed sea state and the forecast skill of wave models, especially in swell-dominated situations [e.g., *Lionello et al.*, 1995]. In particular, this is the case for the world oceans, where the travel time of swell systems can be so long that improving the analyzed model sea state can have an impact for many days

in the forecast. In regional models, the situation is less advantageous. First, wave travel times are much shorter than in the open ocean. Second, the amount of data which is received from satellites is much more limited. Especially, the most detailed data, the two-dimensional wave spectra from the ERS SAR, are measured with an along-track spacing of 200 km, which is very coarse for seas with a typical width of 1000 km or less.

The North Sea forms an exception to this relatively disadvantageous situation. Its dimensions are relatively small (approximately 700 km W-E, 1000 km N-S), but it is open to the Atlantic Ocean in the north. Therefore, in the southern North Sea, swell systems arrive which can be detected up to 2 days in advance at the Norwegian Sea. Furthermore, an important opportunity for data assimilation is created by a network of seven pitch-and-roll (Wavec) buoys, which report detailed information about the directional wave spectrum in near real time to the coast (Figure 1). In addition, over 150 conventional observations of integrated wave parameters (from ships and buoys) are available per day. For

Copyright 1997 by the American Geophysical Union.

Paper number 96JC03242.
0148-0227/97/96JC-03242\$09.00

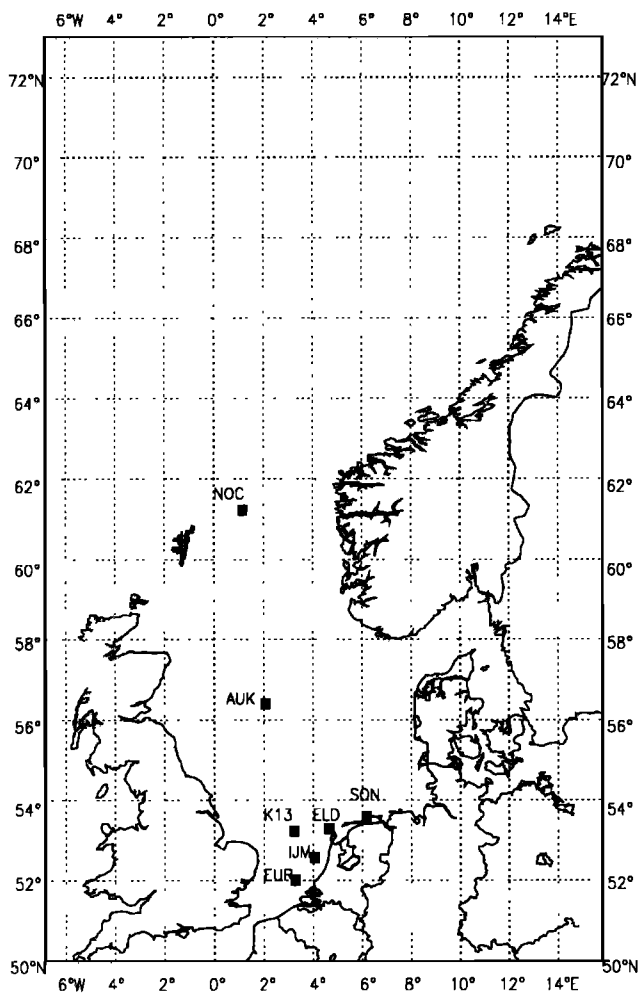


Figure 1. The model region. Indicated are the following Wavec buoy locations: *NOC*, North Cormorant; *AUK*, Auk Alpha; *K13*; *EUR*, Euro Platform; *IJM*, IJmuiden; *ELD*, Eierland; *SON*, Schiermonnikoog Noord.

the North Sea area, this data set is much larger than that from the ERS 1, whose orbit crosses the region only twice a day. The aim of the present paper is to investigate the potential use of the spectral observations from the Wavec buoys for assimilation in an operational forecast system. In a future paper, incorporation of the SAR data will be treated and statistical results from the operational performance of the system will be shown.

Since the first wave data assimilation experiments by *Komen* [1985, 1986], various wave data assimilation methods have been developed. A recent review has been given by *Komen et al.* [1994]. The earlier schemes which were developed were all sequential and time-independent methods [e.g., *Thomas*, 1988; *Esteve*, 1988; *Janssen et al.*, 1989; *Lionello and Janssen*, 1990; *Lionello et al.*, 1992; *Burgers et al.*, 1992; *Lionello et al.*, 1995]. They are computationally cheap, which makes them especially fit for operational use. Later, variational, time-dependent methods have been developed [*de Valk and Calkoen*, 1989; *Monbaliu*, 1992; *Barzel and*

Long, 1994; *de las Heras et al.*, 1994, 1995]. As opposed to the first category, these methods take the model dynamics into account, but at the expense of higher computation requirements. Therefore most of these schemes have been applied either for inverse modeling purposes or for off-line demonstration experiments. An exception is the scheme of *de Valk and Calkoen* [1989]. They use an approximation to the full operational wave model for the minimization of the cost function, which speeds up the procedure at the cost of some accuracy.

Most assimilation schemes which have been tested for operational forecasting, are based on ideas similar to those of *Lionello et al.* [1992] [e.g., *Burgers et al.*, 1992; *Günther et al.*, 1993; *Breivik and Reistad*, 1994]. These schemes are only capable of assimilating observations of the significant wave height (*Burgers et al.* [1992] use also the mean wave period). Until recently, most operationally available observations were indeed wave height data. However, the information contained in wave height observations is often not enough to correct the full two-dimensional wave spectrum [*Mastenbroek et al.*, 1994; *Bidlot et al.*, 1995]. The lack of spectral wave data is probably an important reason why the impact of assimilation on the wave forecast is in general relatively modest.

For the assimilation of two-dimensional inverted wave spectra retrieved from SAR observations, a scheme was developed recently by *Hasselmann et al.* [1994], (*S. Hasselmann et al.*, A wind and wave data assimilation scheme, submitted to *Journal of Geophysical Research*, 1996; hereafter referred to as *Hasselmann et al.* (submitted manuscript, 1996)). The concept of spectral partitioning [*Gerling*, 1992] is used to reduce the number of variables in an optimal interpolation procedure. This makes the scheme efficient and applicable to operational wave forecasting.

In this paper, we adapt the method of *Hasselmann et al.* [1994; submitted manuscript, 1996] in order to assimilate the pitch-and-roll buoy data in the operational North Sea wave model of the Royal Netherlands Meteorological Institute (KNMI). The model is an implementation of the WAM model [*Wave Model Development and Implementation Group*, 1988; *Günther et al.*, 1992; *Komen et al.*, 1994]. A complicating factor is that pitch-and-roll buoys do measure directional information but not the full two-dimensional wave spectrum. The original scheme has been adapted to overcome this difficulty. Also, we discuss problems associated with situations when the number of wave systems in the observation and in the model is different.

First, the scheme is tested in a few identical twin experiments, where the observations are generated by the model itself. Such situations can be examined accurately, since the "truth" is known. Subsequently, we apply the scheme to a recent swell-dominated period, using the available Wavec observations and wind fields from the High Resolution Limited Area Model (HIRLAM) [*Källberg*, 1990]. In all experiments, the re-

sults are compared to those of the scheme of *Burgers et al.* [1992] in order to investigate the effect of directional observations on the wave analysis and forecast.

2. Wave Model

The wave model that we use is the WAM wave model, Cycle 4 [WAMDI Group, 1988; Günther et al., 1992; Komen et al., 1994]. It solves the wave transport equation

$$\frac{\partial F}{\partial t} + \nabla \cdot (\mathbf{c}_g F) = S_{in} + S_{ds} + S_{nl} + S_{bot} \quad (1)$$

where $F(f, \theta, \mathbf{r}, t)$ is the frequency-directional wave variance density spectrum at location \mathbf{r} and time t and $\mathbf{c}_g(D(\mathbf{r}), f)$ is the group velocity depending on the local depth $D(\mathbf{r})$ and frequency f . The right-hand side represents the source terms due to wind input, dissipation through white-capping, nonlinear wave-wave interactions and bottom dissipation, respectively.

The model is implemented on a $1/3^\circ$ latitude \times $1/2^\circ$ longitude grid, which includes the North Sea and part of the Norwegian Sea; see Figure 1. At each grid point, the wave spectrum is discretized in 25 frequencies ranging from 0.04 to 0.4 Hz and in 12 directions.

The main objective of the model is to issue forecasts for the central and southern North Sea. The Norwegian Sea is added to the model domain in order to capture swell which is generated in this area.

3. Observations

Data from seven Wavec buoys in the North Sea (Figure 1) are distributed on a 3-hourly basis via the Dutch measurement network (Meetnet Noordzee). The data arrive within an hour after measurement at KNMI, so that they can be used for operational data assimilation. Especially the data from the northern buoys, near North Cormorant, Auk Alpha, and K13 could be of importance for the 12- to 24-hour forecast near the Dutch coast. Depending on the wave length, the travel time for waves from the most northern observation location (North Cormorant) to the southern North Sea is between 1 and 2 days.

Pitch-and-roll buoys like the Wavec measure directional and spectral information but not the full two-dimensional wave spectrum. The parameters which are reported to KNMI are the wave energy density, mean direction, and directional spread as a function of frequency. Further details are given in subsection 5.3, where the problem is treated how to use this limited amount of spectral information in an assimilation method based on optimal interpolation of spectral wave partitions.

4. Assimilation of Integral Wave Parameters (OI-I)

In this section, we describe briefly a method for the assimilation of observations which are integrated pa-

rameters of the entire wave spectrum: the significant wave height and the mean wave period. We will refer to it as the optimal interpolation of integral wave parameters (OI-I) method. The OI-I scheme will be used as a reference to study the impact of a more sophisticated assimilation scheme which will be presented in section 5. With the latter scheme, it will be possible to assimilate not only integral quantities but also spectral wave observations. We introduce the OI-I scheme first, because it is less complex but has the same structure as the second method. In certain simplified conditions, the two schemes will turn out to be equivalent.

The OI-I method is a straightforward adaptation of the method of *Burgers et al.* [1992]. The adaptations have been applied in order to make it almost equivalent to the new assimilation scheme, in the special case of unimodal wave spectra (e.g., pure wind-sea spectra) for which the mean direction is well represented in the first-guess wave model state.

The assimilation scheme consists of two steps. First, analyzed fields of wave height and wave period are created by optimal interpolation of first-guess and observed parameters (subsections 4.1 and 4.2). Subsequently, the model spectrum and the driving wind are updated locally, based on the analyzed wave height and period and on the first-guess spectrum (subsection 4.3).

4.1. Optimal Interpolation

It is supposed that the only available observations are measurements of the significant wave height

$$H_s = 4\sqrt{E}, \quad (2)$$

where E is the total wave variance

$$E = \int_0^\infty F(f)df, \quad (3)$$

and observations of the mean wave period, which is defined as

$$T_m = \frac{\int_0^\infty F(f)f^{-1}df}{E}. \quad (4)$$

Both parameters can be derived from the one-dimensional energy density spectrum $F(f)$, which is measured by wave buoys.

In contrast to *Burgers et al.* [1992] we do not interpolate wave heights H_s and mean periods T_m directly but instead the total wave energy E and the quantity $k = 1/T_m^2$, which is proportional to the wave number in the deep water limit. This is done in order to keep the model as close as possible to the new assimilation scheme, which will be described in the next section. Analyzed fields of E and k are (independently) obtained using the optimal interpolation step:

$$\mathbf{x}^{an} = \mathbf{x}^{fg} + PH^T [HPH^T + R]^{-1} (\mathbf{y}^{ob} - H\mathbf{x}^{fg}) \quad (5)$$

where \mathbf{x}^{an} (\mathbf{x}^{fg}) is a vector which consists of the analyzed (first-guess) parameter (E or k) at every model

grid point and \mathbf{y}^{ob} is the vector of the corresponding observed values. P and R are, respectively, the forecast and observation error covariance matrices, which have to be prespecified; see subsection 4.2. H is the matrix which projects the model state \mathbf{x} onto the measurement vector \mathbf{y} . In our case, H simply selects the model grid point closest to the observation.

Alternatively, one could choose to interpolate parameters E and k in a multivariate optimal interpolation scheme. This would have the advantage that the correlation between E and k could be taken into account explicitly. We choose, both here and in the OI-P scheme in section 5, the univariate approach because it is simpler and more cost-efficient (the covariance matrices have smaller dimension). Also, the covariance matrices P and R can be determined only approximately because of limited input information (see next subsection). This impedes an accurate determination of the rather subtle effect of cross correlation between E and k .

4.2. Determination of the Error Covariances

For the interpolation (5), the forecast error covariance P and the observation error covariance R have to be prespecified in order to obtain the interpolation weights. Information of these matrices can be obtained by analyzing long-time records of innovations (differences between model and observation), since

$$EV[(\mathbf{y}^{ob} - H\mathbf{x}^{fg})(\mathbf{y}^{ob} - H\mathbf{x}^{fg})^T] = HPH^T + R, \quad (6)$$

where $EV[]$ means taking the expectation value. For the North Sea, an extensive set of buoy measurements is available. The drawback of this set for determining the covariances, however, is the fact that these data come from only seven buoys which are fixed in space. This is insufficient to determine the spatial correlation structure of the innovations. Therefore we will use the buoy data only to obtain the innovation variance. We will use pseudo-“innovations,” which we define as differences between model first-guess and model analysis values, to obtain an estimate of the spatial correlation structure.

We compared 2 years of results of the operational model with observations at North Cormorant, Auk Alpha, K13, Euro Platform, and IJmuiden. After stratifying the data set with respect to total energy, we found for the root-mean-square (RMS) difference of the model and observed energies (in square meters)

$$RMS(E^{fg} - E^{ob}) = 0.03 + 0.50E^{fg} \quad (7)$$

It is difficult to distinguish which part of the RMS difference is due to observation errors and which part is due to forecast errors. Observation errors consist of instrumental errors, errors due to the random variability of the spectrum and limited sample time (see subsection 5.3), and representation errors. Representation error is the difference between what the buoy actually measures (local measurement of the sea state, which is influenced

by sub-grid scale processes as gustiness, influence of local bottom topography, etc.) and its model equivalent, which is a description of the mean sea state over a large area (typically a grid box, i.e., $32 \times 32 \text{ km}^2$). Especially the representation errors are not known accurately. Because of lack of information, we will assume the observation and corresponding forecast errors to be equal. This is a reasonable approximation, since comparison of model and buoy wave heights with an independent data set (the ERS 1 altimeter wave heights) showed scatter values of the same order of magnitude [Mastenbroek *et al.*, 1994].

Thus, with the assumption that the observation error and the error of the corresponding forecast are unbiased and uncorrelated and that their standard deviations are equal,

$$\sigma_{E^{ob}} = \sigma_{E^{fg}}, \quad (8)$$

it follows from (7) that

$$\sigma_{E^{fg}} = 0.02 + 0.35E^{fg}. \quad (9)$$

We assume that the errors of different observations are uncorrelated. R is then a diagonal matrix:

$$R_{ij} = (\sigma_{E^{ob}})^2 \delta_{ij} \quad (10)$$

As stated, the available observations do not allow an accurate estimation of the full forecast error covariance matrix P by analyzing the innovations ($E^{ob} - E^{fg}$). To get an estimate of the spatial correlation structure of the forecast error, we instead analyzed differences between the model analysis E^{+0} and the +24 hours forecast E^{+24} of the operational model, for 2 months of data. Note that in the operational model, no wave observations are assimilated: the model analysis is just a run with analyzed wind fields. Assuming homogeneity and isotropy for the forecast error correlation structure, we fitted a correlation model

$$\rho(\mathbf{r}_1, \mathbf{r}_2) = \exp \left[- \left(\frac{d(\mathbf{r}_1, \mathbf{r}_2)}{L} \right)^a \right] \quad (11)$$

to the “pseudo-innovations” ($E^{+24} - E^{+0}$). Here $d(\mathbf{r}_1, \mathbf{r}_2)$ is the distance between locations \mathbf{r}_1 and \mathbf{r}_2 , L is a correlation length, and a is a power to be estimated. We tried for the latter the values 1, 3/2, and 2. The best fit was found for $a = 3/2$ and $L = 200 \text{ km}$. The forecast error covariance matrix P can now be constructed using (9) and (11):

$$P_{ij} = \sigma_{E^{fg}}(\mathbf{r}_i)\sigma_{E^{fg}}(\mathbf{r}_j)\rho(\mathbf{r}_i, \mathbf{r}_j) \quad (12)$$

For the interpolation of parameter k , we take the same covariance matrices P and R as obtained for E , although this is not based on analysis of long time records of k innovations. The motivation for this choice is that in this way, energy and mean wave number are interpolated in exactly the same manner. This guarantees that the resulting analyzed spectra will have a physi-

cally realistic shape, even in the rather simple univariate optimal interpolation scheme which is used. Different correlation functions for E and k could, for instance, lead to analyzed spectra which are steeper than both the observed and the first-guess spectra.

4.3. Update of the Spectrum and the Wind

After obtaining analyzed fields of $H_s^{an} = 4\sqrt{E^{an}}$ and $T_m^{an} = 1/\sqrt{k^{an}}$, the model spectrum is updated locally at every grid point, using E^{an} , T_m^{an} , and the first-guess spectrum. Following [Burgers *et al.*, 1992], the analyzed wave spectrum is calculated as follows:

$$F^{an}(f, \theta) = \frac{T_m^{an}}{T_m^{fg}} \left(\frac{H_s^{an}}{H_s^{fg}} \right)^2 F^{fg} \left(\frac{T_m^{an}}{T_m^{fg}} f, \theta \right) \quad (13)$$

The first-guess spectrum is considered to be a wind sea spectrum if

$$1.3 \frac{u^{old}}{c_p} \cos(\theta_u - \theta_m) > 1, \quad (14)$$

where u^{old} is the wind speed supplied by the meteorological model; c_p is the phase speed of the waves at the peak of the spectrum, θ_u is the wind direction, and θ_m is the mean wave direction, which is defined as the vectorial mean [Kuik *et al.*, 1988]

$$\theta_m = \arctan \left(\frac{\int \int F(f, \theta) \sin \theta df d\theta}{\int \int F(f, \theta) \cos \theta df d\theta} \right) \quad (15)$$

Only if condition (14) is met is the wind speed updated. This is done in the following way:

$$u^{new} = u^{old} + u^{an} - u^{fg} \quad (16)$$

The wind speeds u^{an} and u^{fg} are calculated from the analyzed and first-guess energy $E^{(r)}$ and mean frequency $f_m^{(r)} = 1/T_m^{(r)}$ ($r = \{an, fg\}$); respectively,

$$\frac{g^2 E^{(r)}}{[u^{(r)}]^4} = A \left[\frac{f_m^{(r)} u^{(r)}}{g} \right]^B \quad (17)$$

where g is the acceleration of gravity, $A = 2 \times 10^{-5}$, and $B = -2.69$. Equation (17) has been obtained by P. Lionello (personal communication, 1995), based on a fit to the WAM growth curve in terms of u_* scaling by Lionello *et al.* [1992]. (Actually, Lionello obtained values of A for 10 m/s and 20 m/s winds. They differ from 2×10^{-5} by approximately 10%. The wind retrieval algorithm uses both values of A to compute the wind speed and interpolates between them to obtain the final wind speed [Hasselmann *et al.*, submitted manuscript, 1996]. The wind speed correction obtained by this procedure is very close to the wind correction obtained with formula (17).)

The new winds are used to force the WAM model for 90 min (half a wind time step), after which the next wind field is read in.

5. Assimilation of Spectral Wave Parameters (OI-P)

The OI-I assimilation method which was described in the previous section can only be used to assimilate significant wave height and mean wave period observations. The limitation of this is twofold. First, there is no possibility to assimilate any measurements of directional wave data. Second, the details of the shape of the wave spectrum (of which the frequency dependence is measured even by nondirectional wave buoys) are not taken into account, so one has to rely entirely on the wave model first-guess spectrum (equation (13)).

In this section, we describe a method with which the more detailed spectral and directional information inferred from pitch-and-roll buoys can be assimilated. The method was developed originally by Hasselmann *et al.* [1994; submitted manuscript, 1996] for the assimilation of inverted two-dimensional wave spectra retrieved from SAR spectra. We adapted the method for pitch-and-roll buoy observations. As will become clear in the sequel, this adaptation is desirable because pitch-and-roll buoy measurements contain very limited information about the directionality of the wave spectrum. Apart from the adaptation to buoy data, some other modifications were made to the Hasselmann scheme, which will be pointed out in the following.

The new assimilation scheme is similar to the OI-I scheme described in section 4, in the sense that it consists of two main steps: first, an optimal interpolation step of some mean parameters of the wave spectrum and, subsequently, a local update of the model wave spectra on the basis of the analyzed parameters and the first-guess spectra. The difference lies in the set of mean parameters. Whereas the OI-I scheme uses only integral parameters over the entire spectrum (wave height and mean period), the new scheme first identifies all independent wave systems ("partitions") present in the spectrum and calculates mean parameters for every partition separately. With this set of parameters, the spectrum can be described with more accuracy than in the OI-I scheme. Although the number of mean parameters which describe the spectrum (around 10) is larger than in the OI-I scheme, it is much smaller than the number of variables in the wave model (300 per spectrum in our implementation of the WAM model). This reduction of variables leads to a gain in efficiency in the optimal interpolation procedure.

In the sequel, we will refer to the new method as optimal interpolation of partitions (OI-P). It will turn out that the OI-I scheme is a special case of the OI-P method: if all spectra consist of only one partition and the mean wave directions of observation and model first guess are the same, the methods are identical.

5.1. Outline of the Method

The assimilation method consists of the following steps, which will all be explained in more detail below.

The first step is the partitioning of all observed and model spectra, i.e., division of each spectrum into a few distinct segments. The physical interpretation of each segment ("partition") is that it represents a wave system, corresponding to a certain meteorological event (swell from a distant storm in the past, wind sea which is generated by local wind). Every partition is described by three mean parameters: its total energy, mean direction and mean frequency.

The cross assignment of partitions of different spectra is the next step: connect partitions which are so close to each other in spectral parameters that they can be supposed to represent the same wave system.

Then, the mean parameters from observed and model partitions which are cross assigned are interpolated by applying an optimal interpolation procedure. Thus an analyzed field of partition parameters is obtained.

Subsequently, each spectrum is updated individually, based on the first-guess spectrum and on the analyzed partition parameters.

Finally, the driving wind field is updated as well, if there is a wind sea-component in the spectrum.

5.2. Spectral Partitioning

The concept of spectral partitioning was introduced by *Gerling* [1992]. It is a method to describe the essential features of a two-dimensional wave spectrum $F(f, \theta)$ with only a few parameters, by separating the spectrum into a small number of distinct segments, so-called partitions. The partitioning is a purely formal procedure; however, the partitions can be interpreted physically as representing independent wave systems.

A partition is defined as the set of all points in the (f, θ) plane which, following the path of steepest ascent in the energy density starting from any of these points, lead to the same local maximum of the energy density spectrum (this is the way *Hasselmann et al.* [1994] calculate the partitions, which is more efficient than the method described by *Gerling* [1992]). Every point in the spectrum is thus assigned to one unique partition. The definition of a partition is analogous to a catchment area in hydrology, if one considers the spectrum as an "inverted" hilly landscape; that is, every local maximum corresponds to a "valley," and to each of them, a partition ("catchment area") belongs.

As said, the physical interpretation of a partition will be that of a wave system, which has a different meteorological origin than other partitions in the spectrum. The data assimilation scheme makes use of this interpretation. The underlying assumption is that components of the discretized spectrum which lie within a partition are fully correlated with each other, whereas components from different partitions are uncorrelated. One can then limit oneself to calculating only a few integrated parameters of every partition and perform the assimilation on these integrated parameters rather than on the full spectrum. The assimilation scheme as designed by *Hasselmann et al.* [1994; submitted

manuscript, 1996] uses three parameters per partition p : the total energy of each partition

$$E_p = \int_{O_p} F(f, \theta) df d\theta, \quad (18)$$

the mean frequency

$$f_{m,p} = \frac{E_p}{\int_{O_p} F(f, \theta) f^{-1} df d\theta}, \quad (19)$$

and the mean direction

$$\theta_{m,p} = \arctan \left(\frac{\int_{O_p} F(f, \theta) \sin \theta df d\theta}{\int_{O_p} F(f, \theta) \cos \theta df d\theta} \right). \quad (20)$$

Here O_p is the part of the spectral domain (f, θ) which belongs to partition p .

Clearly, the assumptions about high correlation of spectral components within a partition, and low correlation between partitions, will be most correct in the case that each partition is "narrow"; that is, most energy within the partition is distributed over a small range of frequencies and propagation directions. This guarantees that the propagation velocity is almost the same everywhere in the partition, so that its total energy will not disperse quickly during propagation. Second, it is important that different partitions are clearly separated in the (f, θ) plane. If not, then the assumption that the partitions are not correlated is obviously incorrect: they will influence each other through the nonlinear wave-wave interactions. Probably, they are generated during the same storm event. Clearly, it is not useful to treat all partitions separately. Therefore partitions are merged together into larger "partitions" if they satisfy one of the following conditions:

1. Two partitions are too close to each other: the distance in the wave number plane between two peaks is smaller than half the spectral width of either one of them.
2. The "contrast" between two peaks is too low: the minimum energy density between two peaks is more than 70% of either of the two maxima.
3. The total energy of a partition is below a threshold value of 0.0025 m^2 .
4. All partitions which are not considered to be swell (see below) are combined into one.

Clearly, the threshold parameters above are rather arbitrary. We have chosen slightly different ones from *Hasselmann et al.* [1994; submitted manuscript, 1996].

Each partition is regarded to be either swell, wind sea, or mixed wind sea/swell. It is considered wind sea if it satisfies (14) (of course the integrals in (15) are now over the partition only, not over the whole spectrum). The partition is considered mixed wind sea/swell if (14) is fulfilled for a "peak frequency" (and corresponding phase speed) and "mean direction" which differ from the actual values by an amount equal to the spread in

direction and frequency of the partition; see also *Hasselmann et al.* [1996]. The remaining partitions are defined as well.

Alternatively, one could devise an optimal interpolation data assimilation scheme directly with the discretized wave spectrum $F(f, \theta)$ instead of the two-step approach using the spectral partitioning parameters. One advantage of the spectral partitioning approach is, as mentioned, the reduction of variables and thus computational efficiency. Another, so far not mentioned strong point of the method is the underlying assumption of high correlation between spectral components within a partition and low correlation between different partitions. The correlation structure between spectral components is thus assumed to be dependent on the wave systems present at a specific time. In a direct optimal interpolation method one would have to prespecify a fixed correlation structure between spectral components, which does less justice to the physical origin of the energy distribution within the spectrum.

5.3. Spectral Observations From Wavec Buoys

As has been pointed out in section 3, pitch-and-roll buoys like the Wavec do not measure the full wave spectrum. Therefore the partitioning scheme described above cannot be applied directly to the buoy data. We will first summarize the parameters which are measured by the buoy, and then adapt the partitioning method to this set of parameters.

5.3.1. Observed parameters. Pitch-and-roll buoys measure the elevation and slope (two directions) of the sea surface as a function of time. From these three time series, one can determine the one-dimensional energy-density spectrum $F(f)$ and some information about the directional distribution of the energy. If one writes the two-dimensional energy density spectrum

$$F(f, \theta) = F(f)D_f(\theta), \quad (21)$$

$$D_f(\theta) = \frac{1}{\pi} \left\{ \frac{1}{2} + \sum_{n=1}^{\infty} [a_n(f) \cos(n\theta) + b_n(f) \sin(n\theta)] \right\}, \quad (22)$$

only the Fourier components for $n = 1, 2$ of the directional distribution can be determined from the auto-spectra and cross spectra of elevation and slope [e.g., *Longuet-Higgins et al.*, 1963]. For convenience, we will drop the frequency dependence of the Fourier components a_n and b_n in the notation below.

One can try to reconstruct the full directional distribution as well as possible based on only these first four Fourier parameters [*Long and Hasselmann*, 1979; *Lygre and Krogstad*, 1986] or fit the data to an assumed shape [*Longuet-Higgins et al.*, 1963]. Subsequently, one could assimilate the full "retrieved" two-dimensional spectra, analogous to the way the SAR spectra are assimilated. The disadvantage of this effort is that, although the obtained spectrum may be "best" according to some

criterion, it suggests much more knowledge about the spectrum than what is actually measured. Errors in the various components of the "reconstructed" spectrum will necessarily be strongly correlated, which obscures the comparison with, e.g., a spectrum obtained from a wave forecast model at the same place and time.

The same objections could be raised to the SAR inversion/assimilation procedure. The nature of the SAR data, however, is quite different from the buoy data. First, the SAR observations themselves are strongly nonlinearly distorted images of the wave spectrum, so direct assimilation in an optimal interpolation scheme seems impossible here. Second, the long wave part of the inverted SAR spectrum (which is the most interesting part for assimilation purposes, because it contains mostly swell) seems to be only weakly dependent on external (model first guess) information [*Brüning and Hasselmann*, 1994]. Pitch-and-roll buoys measure the directionality of the wave spectrum relatively crudely, so more external information has to be added for the low frequencies in an "inversion" procedure.

Instead of constructing the whole directional spectrum, we will use only the one-dimensional energy density spectrum $F(f)$ and some mean parameters for each frequency band, which are uniquely determined by the first few Fourier components. We follow *Kuik et al.* [1988] by defining the mean direction

$$\theta_0 = \arctan(b_1/a_1). \quad (23)$$

For graphical presentation of the spectra we will also use a measure for the angular spread,

$$\Delta\theta = 2(1 - \sqrt{a_1^2 + b_1^2}). \quad (24)$$

Kuik et al. [1988] discuss other definitions of the angular spread but choose (24) since it best approaches the standard deviation of the energy for narrow and symmetrical beams. The four Fourier components further allow definition of third- and fourth-order angular moments (skewness and kurtosis). We shall not discuss them here. Generally, one can conclude that the accuracy of estimated moments quickly decreases with increasing order (see, again, *Kuik et al.* [1988]).

In the assimilation procedure, we will use only $F(f)$ and $\theta_0(f)$. These parameters are measured with limited accuracy due to random variability of the spectrum and the limited sample interval. Let T be the total sample period and $\delta f = 1/T$ be the frequency spacing of the discrete Fourier transform. The standard deviation σ_F of the estimate of $F(f)$ averaged over a bandwidth Δf is given by [e.g., *Tucker*, 1991]

$$\frac{\sigma_F}{F(f)} = \sqrt{\frac{2}{\mu}} \quad (25)$$

The error σ_{θ_0} in $\theta_0(f)$ is approximately [*Kuik et al.*, 1988]

$$\sigma_{\theta_0(f)} = \sqrt{\frac{1}{\mu} \left(\frac{2\Delta\theta}{2 - (\Delta\theta)^2} \right)} \quad (26)$$

Here μ is the so-called “effective” number of degrees of freedom. If F is white over Δf , then $\mu = 2\Delta f/\delta f$. If the spectrum has a typical spectral width Δf_{eff} which is smaller than Δf , then μ reduces to $2\Delta f_{\text{eff}}/\delta f$.

The buoy spectra that we use are determined from six measurement records of 200-s length and are compressed into spectral bands of 10 mHz, giving 24° of freedom per frequency band. Thus the relative error in energy due to random variability is 29% for a 10-mHz band. For a spectrum with a typical width of 100 mHz, $\mu = 240$ and the accuracy of the total energy estimate is approximately 10%. For the estimate of the mean direction of a spectrum with a typical angular spread of 30° , the errors are 7° for a 10-mHz band and 2.2° for $\Delta f_{\text{eff}} = 100$ mHz. As already mentioned in subsection 4.2, these sample errors are estimated to be smaller than the representation errors.

5.3.2. Partitioning of buoy spectra. For the assimilation of pitch-and-roll buoy data, one option is to apply the original partitioning scheme of subsection 5.2 to a “reconstructed” full wave spectrum. We, however, prefer to use only the truly observed parameters and devise a new partitioning scheme based on these data. Of course, the new scheme should stay as close as possible to the partitioning scheme for the full spectrum.

The scheme uses only the energy-density spectrum $F(f)$ and the mean direction $\theta_0(f)$, as defined in (23). It consists of the following subsequent partitioning/recombination steps:

1. The one-dimensional spectrum $F(f)$ is partitioned. This step is formally the same as the partitioning of the two-dimensional spectrum, but much easier in one dimension.

2. The partitions are combined under the following conditions. First, if two maxima are separated less than half the width at half maximum of either of the two peaks. Second, if the minimum energy density between two neighboring maxima is more than 50% of the minimum energy density of either one of the maxima. Note that this is the one-dimensional energy density $F(f)$ instead of the two-dimensional density $F(f, \theta)$ which is used in the previous subsection. Therefore this is a different “contrast”, and the threshold value has to be retuned by trial and error. The final condition for combining of partitions is if the total energy of a partition is less than 0.0025 m^2 .

3. New partitions are defined when the mean direction changes fast with frequency within a partition: when the mean direction differs more than 50° from the mean direction at the peak of the partition, a new partition is created.

4. All partitions which are wind sea or mixed wind sea/swell according to criterion (14) are recombined into one partition.

The mean direction $\theta_m^{(1D)}$ of the thus obtained partitions is calculated as follows:

$$\theta_m^{(1D)} = \arctan \left(\frac{\int_{f_{\min}}^{f_{\max}} df F(f) \sin \theta_0(f)}{\int_{f_{\min}}^{f_{\max}} df F(f) \cos \theta_0(f)} \right), \quad (27)$$

where f_{\min} and f_{\max} are the lower and upper frequency bounds of the partition.

The method is a rather ad hoc adaptation of the full partitioning for the two-dimensional spectra. We checked its quality by the following procedure. We extracted from a number of wave model (two-dimensional) spectra the pitch-and-roll buoy parameters $F(f)$, $\theta_0(f)$. We applied the full partitioning scheme directly to the two-dimensional WAM spectrum and the new partitioning scheme to the extracted buoy parameters. In most cases, we found a very good agreement between resulting partitions of the two schemes. Exceptions were formed by the few spectra where two wave systems were present with different mean directions, but with approximately the same mean frequencies: here the wave systems cannot be separated if one only knows the mean direction and not the directional distribution as a function of frequency.

5.4. Cross Assignment of Wave Partitions

The next step in the assimilation procedure is to merge the model first-guess and observed partition parameters into an analyzed field of parameters. We have assumed that different partitions within a spectrum are uncorrelated, since they are created by different meteorological events. So, we want to treat these partitions separately from each other in the assimilation. On the other hand, partitions in different spectra (e.g., model and observed spectra or two model spectra at different locations) are correlated if they are created by the same event. Therefore we have to define a cross assignment criterion between the partitions of two different spectra, in order to decide whether a partition in one spectrum represents the same wave system as a partition in the other spectrum.

Suppose we have two spectra A and B with n_A and n_B partitions, respectively. Then, for every partition $i(A) = 1, \dots, n_A$ of A , the procedure to select a partition $j(B)$ of B to be cross assigned to is the following:

1. The mean coordinates of the two partitions $i(A)$ and $j(B)$ must be within some distance of each other in the wavenumber spectrum: the distance is defined such that the maximum difference in mean direction is 50° for equal mean frequencies or a difference of 40% in mean frequency if the directions are the same.

2. The energy of one partition is at least 5% of the other.

3. The partitions must be wave systems of the same type, i.e., both wind sea or both swell.

4. If several partitions of spectrum B fulfill the above

conditions, the one which is closest in wave number is chosen.

We denote the results of the cross assignment procedure in the following way: $\delta_{i(A)j(B)} = 1$ if partitions $i(A)$ and $j(B)$ are cross assigned and $\delta_{i(A)j(B)} = 0$ if they are not. Every partition is assigned to at most one partition of the other spectrum. The problems which arise when a partition is not assigned to any partition will be discussed in subsection 5.6.

5.5. Optimal Interpolation of Wave Partitions

When the cross assignment is done, the mean parameters of the model and observed partitions can be combined to obtain an analyzed field of partition parameters. Like in the assimilation procedure of the previous section, the mean parameters are treated separately. Since a direction is not a convenient parameter for interpolation due to its periodicity, we take as mean parameters the combination $k_{x,p}, k_{y,p}, E_p$ instead of $f_{m,p}, \theta_{m,p}, E_p$, where

$$k_{x,p} = f_{m,p}^2 \cos \theta_{m,p} \quad (28)$$

$$k_{y,p} = f_{m,p}^2 \sin \theta_{m,p} \quad (29)$$

are proportional to the deep water wave number components.

To obtain the desired analyzed field of partition parameters, we can apply the following optimal interpolation-like step on the cross assigned partitions:

$$\mathbf{x}_{\mathbf{r},p(\mathbf{r})}^{an} = \mathbf{x}_{\mathbf{r},p(\mathbf{r})}^{fg} + \sum_{\mathbf{r}^{ob}} W_{\mathbf{r},\mathbf{r}^{ob}} \left\{ \sum_{p(\mathbf{r}^{ob}),q(\mathbf{r}^{ob})} \delta_{p(\mathbf{r}^{ob})q(\mathbf{r}^{ob})} \delta_{p(\mathbf{r})p(\mathbf{r}^{ob})} [\mathbf{y}_{\mathbf{r}^{ob},q(\mathbf{r}^{ob})} - \mathbf{x}_{\mathbf{r}^{ob},p(\mathbf{r}^{ob})}] \right\} \quad (30)$$

Here \mathbf{x}^{an} and \mathbf{x}^{fg} are the analyzed and first-guess vectors of any of the three mean partition parameters, subscript \mathbf{r} gives the position in the model grid, and $p(\mathbf{r})$ numbers the partitions within the spectrum. Furthermore, \mathbf{y} is the observation vector, subscript \mathbf{r}^{ob} denotes the location of the observed spectrum, and $q(\mathbf{r}^{ob})$ numbers the partitions of the observed spectrum (note that for simplicity, we assume in (30) that the observation location is equal to that of a model grid point).

Two cross assignments have to be made. The first is between observed and model spectra at the observation sites and is denoted with $\delta_{p(\mathbf{r}^{ob})q(\mathbf{r}^{ob})}$. This function, multiplied with the difference between model and observed partition parameters ($\mathbf{y}_{\mathbf{r}^{ob},q(\mathbf{r}^{ob})} - \mathbf{x}_{\mathbf{r}^{ob},p(\mathbf{r}^{ob})}$), gives the set of innovations. The second cross assignment $\delta_{p(\mathbf{r})p(\mathbf{r}^{ob})}$ is done between model spectra at every grid point and the model spectra at the observation points only. This cross assignment is done to ensure that only the innovations corresponding to the same wave system add to the correction of a model partition. Instead of $\delta_{p(\mathbf{r})p(\mathbf{r}^{ob})}$, one could also choose to use $\delta_{p(\mathbf{r})q(\mathbf{r}^{ob})}$, which is actually done in the original scheme

of *Hasselmann et al.* [1994]. However, we found the present choice to be more robust, because two model spectra are generally more similar than a model and an observed spectrum.

The optimal interpolation weight factor $W_{\mathbf{r},\mathbf{r}^{ob}}$, finally, is determined by the error covariances:

$$W_{\mathbf{r},\mathbf{r}^{ob}} = [PH^T(HPH^T + R)^{-1}]_{\mathbf{r},\mathbf{r}^{ob}} \quad (31)$$

P and R are the model first-guess and observation error covariance matrices. In principle, the errors (and so the weight W) depend not only on the position but also on the partition, but the latter dependence is dropped for simplicity. Therefore P is an $n \times n$ matrix and R is an $m \times m$ matrix, where n is the number of model grid points and m is the number of observed spectra. H is the projection from model position onto observation position (which is trivial since we assumed that the observation is done at a model grid point). For P and R , we assume exactly the same form as in the assimilation scheme of section 4, as given by (10) and (12).

Comparison of (30) and (31) with (5) shows that the optimal interpolation steps for OI-I and OI-P are equivalent in the case that all spectra consist of only one partition, all partitions of the observed and model spectra are cross assigned ($\delta_{p(\mathbf{r}^{ob})q(\mathbf{r}^{ob})} = 1$ and $\delta_{p(\mathbf{r})p(\mathbf{r}^{ob})} = 1$), and the mean directions of observed and corresponding model spectra are equal.

5.6. Treatment of Nonassigned Partitions

A fundamental problem of the method is that the number of partitions in one spectrum is not necessarily equal in every spectrum, and even if two spectra do have the same number of partitions, it is possible that not every partition of one spectrum can be cross assigned to a partition in the other spectrum. The question is what to do with the nonassigned partitions in the optimal interpolation. We have chosen the following solution.

The first cross assignment step in the optimal interpolation (30) is between model and observed spectra at the observation sites, to obtain $\delta_{p(\mathbf{r}^{ob})q(\mathbf{r}^{ob})}$. If a partition is present in the first-guess but not in the observation, we simply interpret this as an observation of the partition with zero energy at the same frequency and direction. For the OI of energy, this leads to an innovation $(0 - E_p^{fg})$, which will be interpolated to the vicinity of the observation point.

If a partition is present in the observation but not in the first guess, it is more difficult to incorporate it in a sensible way. *Hasselmann et al.* [1994] choose to simply superimpose the observed partition, scaled with the OI weight factor of (31), onto the analyzed wave spectra which result from the assimilation procedure. In the case of pitch-and-roll buoy observations instead of SAR observations, this is not directly possible, because the exact two-dimensional energy distribution of the observed partition is not known. Furthermore, it is a rather ad hoc solution which is not entirely consis-

tent with the general approach of adapting first-guess partitions in the spectrum.

Therefore we choose a different approach in the case that an observed partition cannot be matched to a partition of the first-guess spectrum at the observation point. First, we try to merge the observed partition with another observed partition which is not too much different in frequency and direction but is more different than was allowed in the original partitioning/combination procedure. We apply the rather arbitrary conditions that the mean directions must differ less than 90° and the mean frequencies less than 300 mHz. If even this very crude combination of observed partitions is not possible, we discard the observed spectrum from the assimilation. Although this may not be the optimal choice, it is robust: it is better to discard some good observations than to use some data in a wrong way.

After these two steps, all innovations are clearly defined. The second cross assignment in (30), between model spectra at all model locations \mathbf{r} and model spectra at observation locations \mathbf{r}^{ob} , simply selects those innovations which correspond to a certain model partition. No additional decisions concerning nonassigned partitions have to be made, and (30) can be applied directly.

5.7. Update of the Spectrum and the Wind Field

The analyzed partition parameters from the optimal interpolation (30) are now combined with the first-guess spectra to obtain analyzed spectra. Every first-guess partition is multiplied by a scale factor and shifted in the (f, θ) plane such that its mean parameters E_p , $f_{m,p}$, and $\theta_{m,p}$ are equal to the parameters obtained by the optimal interpolation:

$$F^{an}(f, \theta) = \sum_p \left\{ \delta_{(f-\Delta f_p, \theta-\Delta \theta_p); O_p} F^{fg}(f - \Delta f_p, \theta - \Delta \theta_p) \frac{E_p^{an}}{E_p^{fg}} \frac{f - \Delta f_p}{f} \right\} \quad (32)$$

with

$$\delta_{(f-\Delta f_p, \theta-\Delta \theta_p); O_p} = \begin{cases} 1 & \text{if } (f - \Delta f_p, \theta - \Delta \theta_p) \in O_p \\ 0 & \text{otherwise} \end{cases} \quad (33)$$

where $\Delta f_p = f_{m,p}^{an} - f_{m,p}^{fg}$ and $\Delta \theta_p = \theta_{m,p}^{an} - \theta_{m,p}^{fg}$ are the OI increments of mean frequency and mean direction of partition p , respectively. Small gaps in the spectrum which arise by the different shifts for different partitions are filled by two-dimensional parabolic interpolation.

When a wind sea partition is present in the spectrum, the driving wind field is modified using (16) and (17). The new winds are used until the next wind field is read in, which is half a wind time step later (90 min).

6. Experiments With Synthetic Data

6.1. Test Cases

In this section, assimilation experiments are described in which the truth is known; that is, it is generated by a model run. Observations are extracted from the “true” run and assimilated in a “first-guess” model run, which differs from the true run because the driving wind field is different. Knowing the truth, it is possible to determine exactly the effect of assimilation in these idealized cases.

In the first test case, hereafter referred to as experiment S1, the equivalence of the two previously described assimilation schemes is tested in the case of unimodal wave spectra. The true wind field is a homogeneous northerly wind in the northern part of the model, which generates pure northerly swell in the southern part. The first-guess field underestimates the wind in the northern part; see Table 1.

The second and third experiment, S2 and S3, again are runs with a very schematic wind field (Table 1). However, they qualitatively simulate a situation in the southern North Sea which occurs regularly. The wave field in the southern North Sea consists of two wave systems with clearly different origin: one locally generated wind sea component (propagating to the northeast) and a swell component which is generated by northern wind in the northern part of the model region. In S2, the local wind field in the south is overestimated. In S3,

Table 1. Driving Wind Fields for the Synthetic Experiments

Case	True Wind				First-Guess Wind			
	North		South		North		South	
	Speed, m/s	Direction	Speed, m/s	Direction	Speed, m/s	Direction	Speed, m/s	Direction
S1	15	N	0		10	N	0	
S2	15	N	10	SW	15	N	12	SW
S3	15	N	10	SW	10	N	12	SW

“North” columns give the wind speed and direction at 58° N latitude and higher; “South” columns give the wind velocity below 58° latitude. “N” is northerly wind; “SW” is southwesterly wind.

the swell in the south is underestimated because the northerly wind in the north is underestimated.

In all the experiments, the wind field is constant in time. The first-guess run (which we refer to as NOASS (no assimilation) run) and truth run are spun up for a period of 72 hours, until a steady state is reached. From the model spectra of the truth run, synthetic pitch-and-roll buoy observations are extracted at the platform locations which are indicated in Figure 1. No observational noise is added. Therefore in the assimilation experiments the error in the observations is assumed to be 0, in contrast to the assumption (8), which is only used for experiments with real data. From the steady state NOASS solution, assimilation runs of 48 hours are performed, with an assimilation interval of 3 hours. The OI-I scheme assimilates wave height and mean period observations at the given locations, the OI-P scheme assimilates the full pitch-and-roll buoy observations (energy and mean direction as function of frequency). Forecast runs are performed from the analyzed sea state after 24 hours of assimilation in order to assess the impact of the assimilation on the forecast.

6.2. Results

6.2.1. Pure swell (S1). Figure 2 shows the constant first-guess and true wind and wave height fields for experiment S1. The underestimated first-guess wind in the northern part of the model creates too low wind sea in the north and too low swell in the south. Figure 3 shows time series of significant wave height H_s and mean period T_m for the locations North Cormorant, Auk Alpha, and K13. At all observation locations, H_s and T_m are corrected to the true value after the first assimilation. In North Cormorant, H_s drops quickly back to the NOASS value until it is updated at the next assimilation step. The reason of this quick loss of information is that no observations “upstream” (more northern than North Cormorant) are available, so that all the information obtained at the first assimilation step propagates away from the platform. At Auk Alpha, the same happens the first two or three assimilation times; but after this, the information from the North Cormorant observations has propagated southward, resulting in a more stable signal at Auk Alpha. At K13, the equilibrium sets in even quicker because of the vicinity of Auk Alpha. Both assimilation schemes produce almost exactly the same results, which confirms the equivalence of the schemes in the case of unimodal wave spectra of which the first-guess mean direction is close to the truth.

The true sea state is reconstructed almost exactly at the observation sites, but this is not the case at other locations. Even after a steady state has been reached, the wave field away from the observations is not correct. Evidently, this is partly so because the observations simply do not contain information about the whole model area: especially, upstream of the first ob-

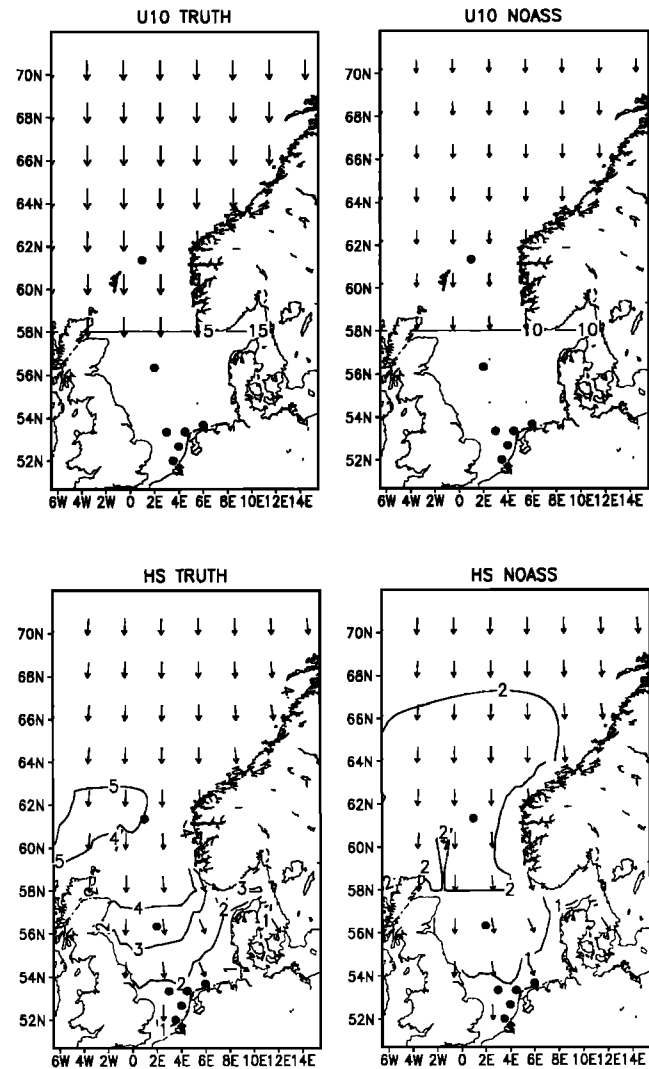


Figure 2. (Left) true and (right) first-guess wind and wave fields for experiment S1. The top panels show the wind fields. Contours show the wind speed; arrows show wind direction. The bottom panels are the wave fields. Contours show the significant wave height; arrows show the mean wave direction.

ervation site (North Cormorant), no “true” data are available. But another reason is that the optimal interpolation scheme is not taking into account the model dynamics. We illustrate this problem by assimilating only the North Cormorant data. Figure 4 shows the difference in wave height and mean period between the truth and the OI-I assimilation run (OI-P gives equivalent results) after the first, third, and last (48 hours) assimilation. After the first assimilation, one sees that the wave field is corrected symmetrically around the observation sites, caused by the assumed isotropic forecast error correlation in the assimilation procedure. At North Cormorant, the model value is equal to the observation; everywhere else it is lower, since the first-guess values are lower than the truth. After more assimilation steps, however, the correction is largest somewhat

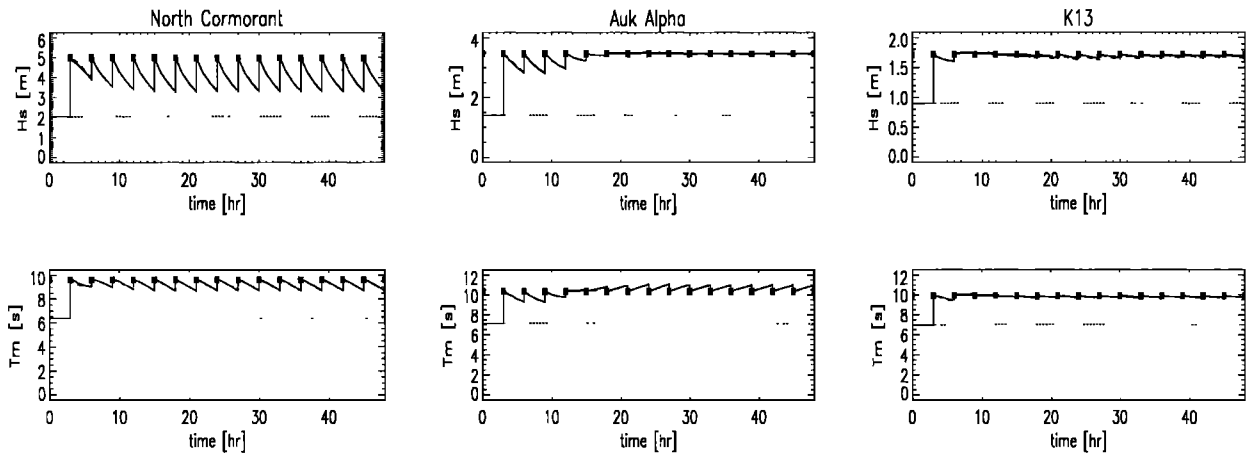


Figure 3. Time series of significant wave height and mean wave period for experiment S1: (left) North Cormorant; (middle) Auk Alpha; (right) K13. Boxes, observations (true values); dotted lines, no assimilation (NOASS); dashed lines, OI-I; solid lines, OI-P. The OI-I and OI-P curves are hardly distinguishable in this experiment.

downstream of the observation sites due to propagation of prior information. Clearly, the maximum correction lies south of North Cormorant. At this point, the wave height and period are overcorrected; that is, their values are higher than the true values. This overcompensation is a fundamental weakness of the optimal interpolation procedure. The scheme ignores the fact that the forecast error is reduced in the vicinity of the observation after assimilation, and moreover, it neglects the propagation of the information to the south. Just before the next assimilation time, the model state will be most accurate south of North Cormorant, which is not represented by the forecast error covariance matrix of the assimilation scheme. This weakness can only be removed by calculating the forecast error covariance dynamics explicitly with, e.g., a Kalman filter or implicitly with the adjoint method.

The problem is largest when there are frequent observations at few, constant positions, which are heavily weighted in the OI procedure. If the time between two assimilations is large, the area with increased accuracy will have propagated away from the region of influence of the observation before the next assimilation. If there are many observation locations, the overcorrected model state can be drawn back to the true state by observations “downstream.” So the problem is larger when only the North Cormorant data are assimilated, than when all seven buoys are used.

Figure 5 shows 24-hour forecasts after 24 hours of assimilation of data from all seven buoys. At North Cormorant, the most northern location, the impact of assimilation on the forecast is lost within 12 hours. In the southern North Sea, however, the forecast is improved for over 24 hours. This illustrates the potential use of data assimilation for swell forecasting in the North Sea region, given the present set of observations.

6.2.2. Bimodal wave spectra: Overestimation of wind sea (S2).

Experiment S2 simulates a case in which a northerly swell is modeled well but the local wind is overestimated in the southern North Sea (see Table 1 for the wind fields). Figure 6 shows assimilation results for two observation locations. Although both assimilation schemes correct the wave height equally well, the OI-P scheme is clearly superior in adjusting the mean wave direction. This is better illustrated in Figure 7, which shows the true, first-guess, and analyzed spectra at K13 after the first assimilation time. OI-P recognizes that only the wind sea is overestimated in the first guess and leaves the swell part unchanged. OI-I reduces the total energy of the first-guess spectrum to the observed energy but keeps the energy distribution between swell and wind sea constant. This results in a spectrum with a too low swell and a too high wind sea partition. Even an extended assimilation period does not result in a realistic wave spectrum.

In a forecast after the assimilation (not shown), the model appeared to relax back to the NOASS state within a few hours. This is due to the fact that it is the wind sea which was corrected in the southern North Sea; as soon as the model is driven by the wrong wind speed again, the waves quickly relax back to the first-guess solution.

6.2.3. Bimodal wave spectra: Underestimation of swell (S3).

The last experiment, S3, simulates a common situation in operational North Sea wave forecasting: the local wind sea in the southern North Sea is modeled reasonably well, but swell from the north is underestimated by the model (see Table 1). Figure 8 shows analyses at some platforms. Again, it is seen that OI-P reconstructs the mean direction much better than OI-I. Nevertheless, it appears now that also OI-I converges to the correct solution, albeit only after more

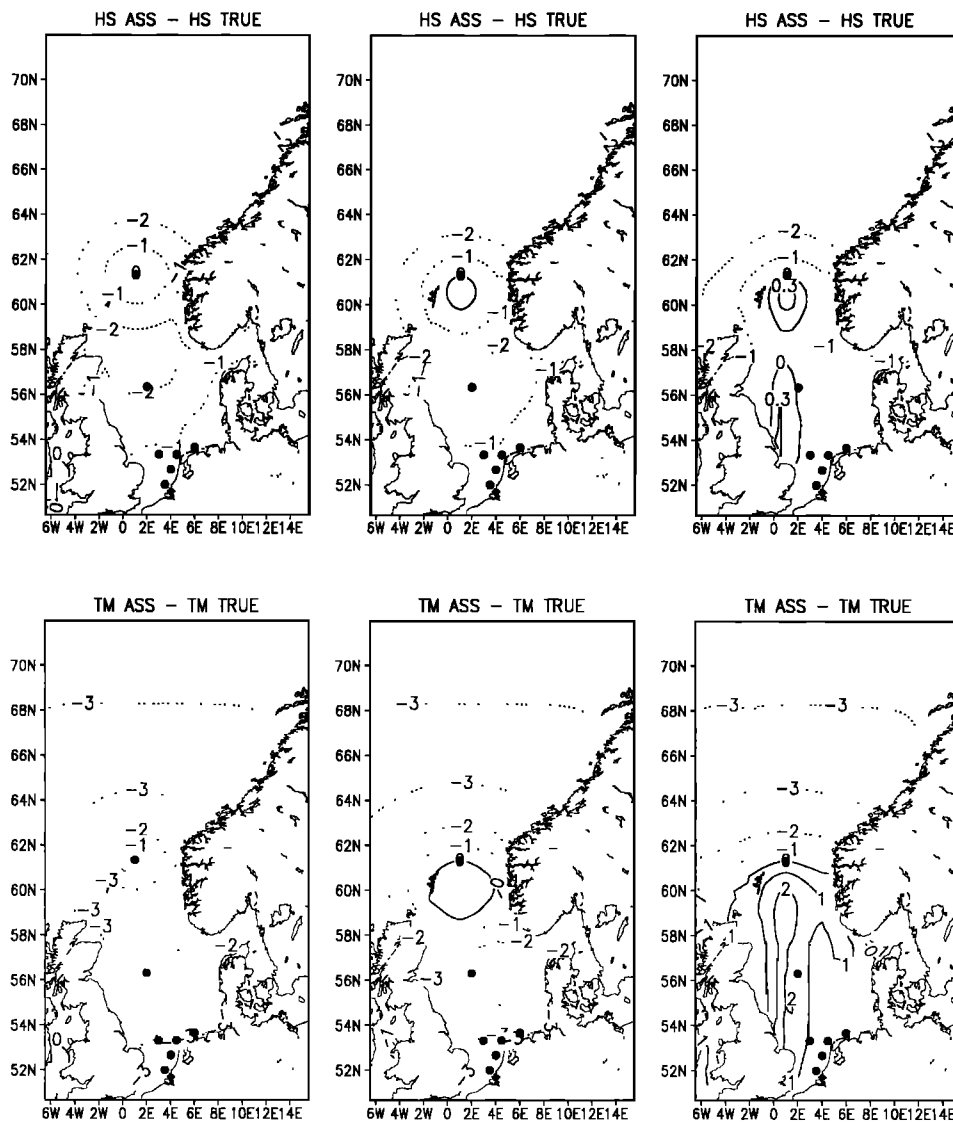


Figure 4. Assimilation-minus-truth wave height and wave period fields after (left) one, (middle) three and (right) 16 assimilation steps for experiment S1, with assimilation only at North Cormorant. The top panels show wave height; the bottom panels show mean wave period.

than 24 hours of assimilation. The reason for this can be understood as follows. After the first assimilation by OI-I, the (too low) swell partition and the (correct) wind sea partition are increased in energy by the same amount in order to correct the total energy. In the next 3 hours, the wind sea quickly drops because it is too high for the driving wind, but the swell decays much slower. So after 3 hours the fraction of the total energy which is contained in the swell is higher than 3 hours before. Again, the energy of the swell and the wind sea peak are increased with an equal factor, and the wind sea decays faster than the swell peak. After many assimilation steps, this procedure eventually leads to the right distribution of energy between the two partitions.

In the northern part of the model, assimilation with the OI-I scheme leads to an unstable phenomenon, as can be seen from Figures 9 and 10. Exactly the reverse

of the mechanism described above applies here. In Figure 10 it is shown that at North Cormorant, a tiny swell system coming from the south is present in the first-guess spectrum, which has been generated by the SW winds in the southern and central North Sea. OI-I increases both the local wind sea and the swell because of the too low wave energy in the first guess. In the 3 hours after, the large wind sea peak decays much faster than the swell peak because of the too low driving wind. The erroneously increased swell peak is again increased at the next assimilation step. This process repeats itself, and already after five assimilation steps (i.e., after 15 hours) a totally incorrect wave spectrum results (Figure 10). This catastrophic behavior does not show up in the OI-P assimilation, because it correctly identifies the various partitions. The swell which is generated by the OI-I scheme at North Cormorant propagates to the

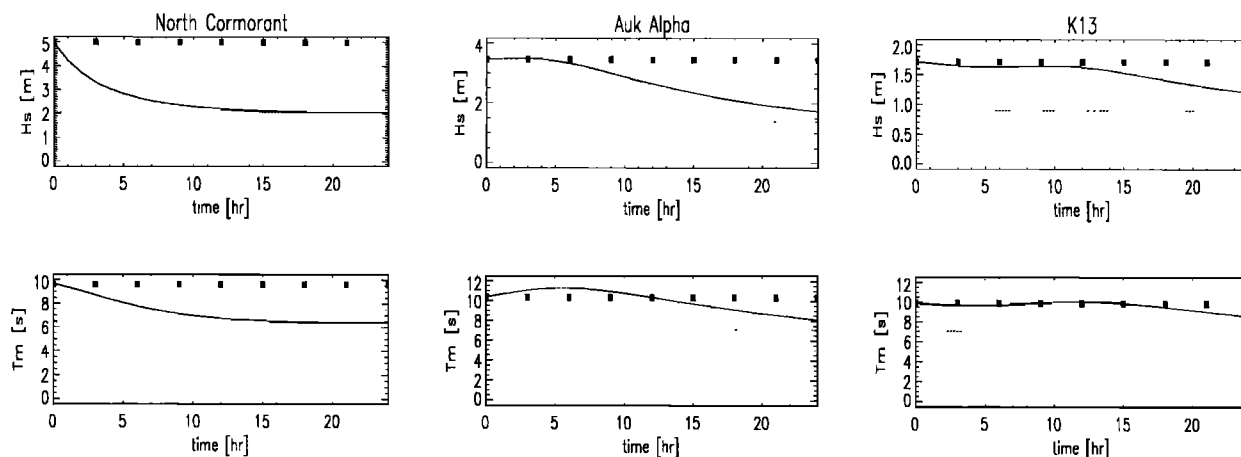


Figure 5. Time series showing the impact of assimilation on the forecast in experiment S1: (left) North Cormorant; (middle) Auk Alpha; (right) K13. The top panels show significant wave height. The bottom panels show mean wave period. Boxes, observations (truth); dotted line, NOASS; solid line, forecast after 24 hours of OI-I or OI-P assimilation.

north, which leads to a strongly disturbed wave height field in the Norwegian Sea after a day, as can be seen from Figure 9.

7. Hindcasts With Real Data

7.1. Description of the Selected Period

The period which we selected for testing the assimilation schemes is May 12–16, 1993, which was characterized by very quiet weather in the southern North Sea but relatively strong northern winds (up to 15 m/s) in

the southern Norwegian Sea, resulting in moderate but clearly distinguishable swell in the North Sea. It is a situation in which data assimilation could be of value both for analysis and for forecast, the latter because of the long travel time of swell to the Dutch coast after passing the northern observation locations.

Figure 11 shows a sequence of wind fields, which are supplied by KNMI's operational atmospheric limited area model, the HIRLAM model [Källberg, 1990]. One can roughly distinguish three periods. At May 12 and 13, the northerly wind in the south Norwegian Sea grad-

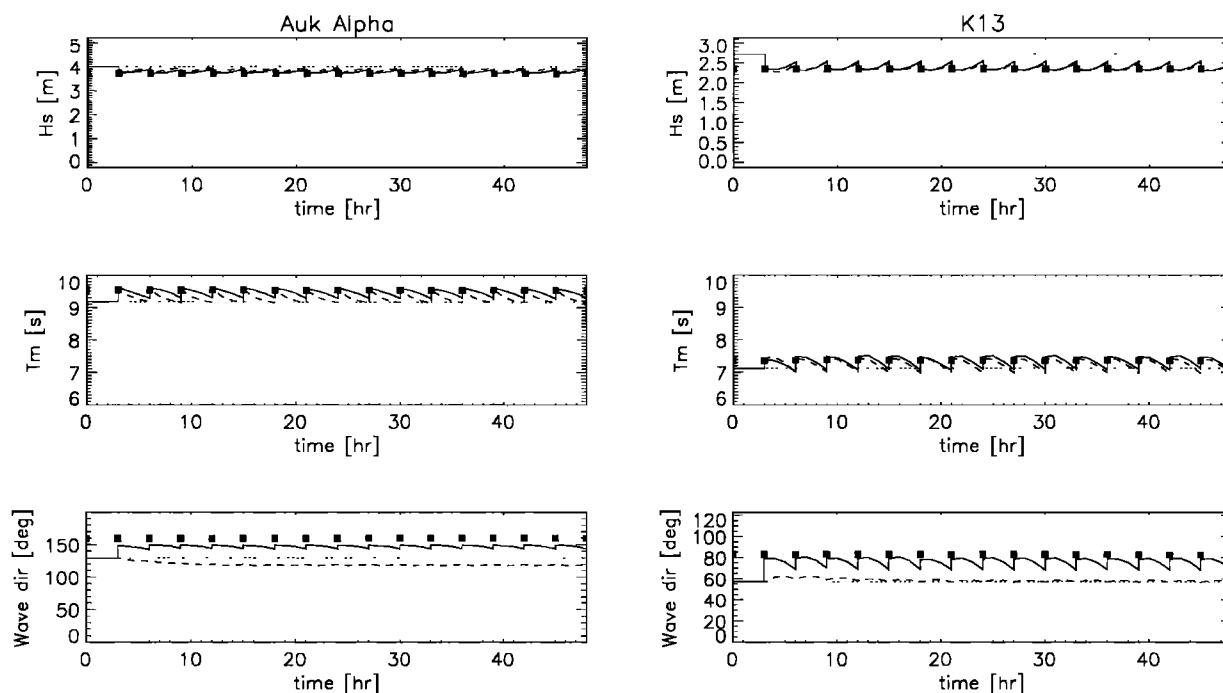


Figure 6. Time series of (top) significant wave height, (middle) mean wave period, and (bottom) mean wave direction for experiment S2 at (left) Auk Alpha and (right) K13. Boxes, observations (true values); dotted line, no assimilation (NOASS); dashed line, OI-I; solid line, OI-P.

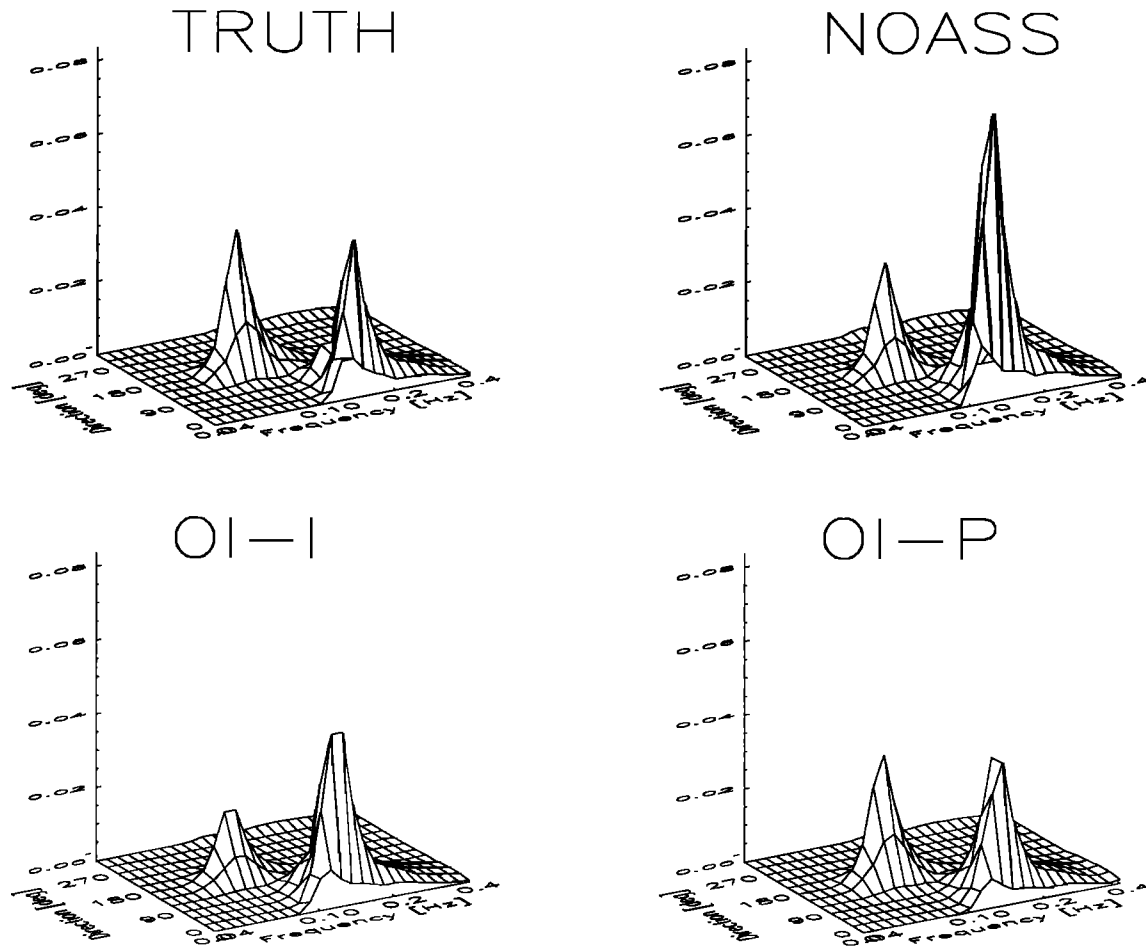


Figure 7. Wave spectra at K13 for experiment S2. The top left panel shows the true wave spectrum. The top right panel shows the NOASS spectrum. The bottom left panel shows the spectrum after the first assimilation with the OI-I scheme. The bottom right panel shows the spectrum after the first assimilation with the OI-P scheme.

ually builds up, while the wind in the southern North Sea turns from east to north. At May 14, the wind in the southern North Sea drops and turns to east and later to south, and the wind in the northern North Sea remains more or less constant. This is a period when swell from the north and local wind sea can be expected simultaneously near the Dutch coast. On May 15, finally, the wind near Scotland turns more to the east and a southwestern wind dominates in the North Sea.

Three wave model runs have been done during this period, using the HIRLAM analyzed wind fields. In the first run (NOASS), no wave data were assimilated; in the other two, 3-hourly observations of Wavec buoys were assimilated with the OI-I scheme (only H_s and T_m) and with the OI-P scheme (spectra), respectively. Wave data have been assimilated for all buoys indicated in Figure 1 except for North Cormorant, from which no data are available for the period of interest. Observations and first-guess values have been given equal weights in the assimilation schemes, as specified in (8) and (9).

In order to study the impact of the assimilation on the forecast, two 24-hour “forecast” runs have been carried out, starting from the analyzed wave fields obtained with the assimilation schemes. In these runs, the analyzed HIRLAM fields have been used, but no wave data have been assimilated. Consequently, these runs finally converge to the NOASS run.

7.2. Results

Figure 12 shows time series of the three analysis runs for locations Auk Alpha (central North Sea) and IJmuiden (Dutch coast) of mean direction, mean period, and the low-frequency wave height H_7 , which is defined as

$$H_7 = 4 \sqrt{\int_0^{\frac{1}{7} H_z} F(f) df}. \quad (34)$$

The first striking feature that can be noted is the systematic underprediction of wave height by the NOASS run at both locations, during most of the 4-day period. Both assimilation schemes correct the wave height quite

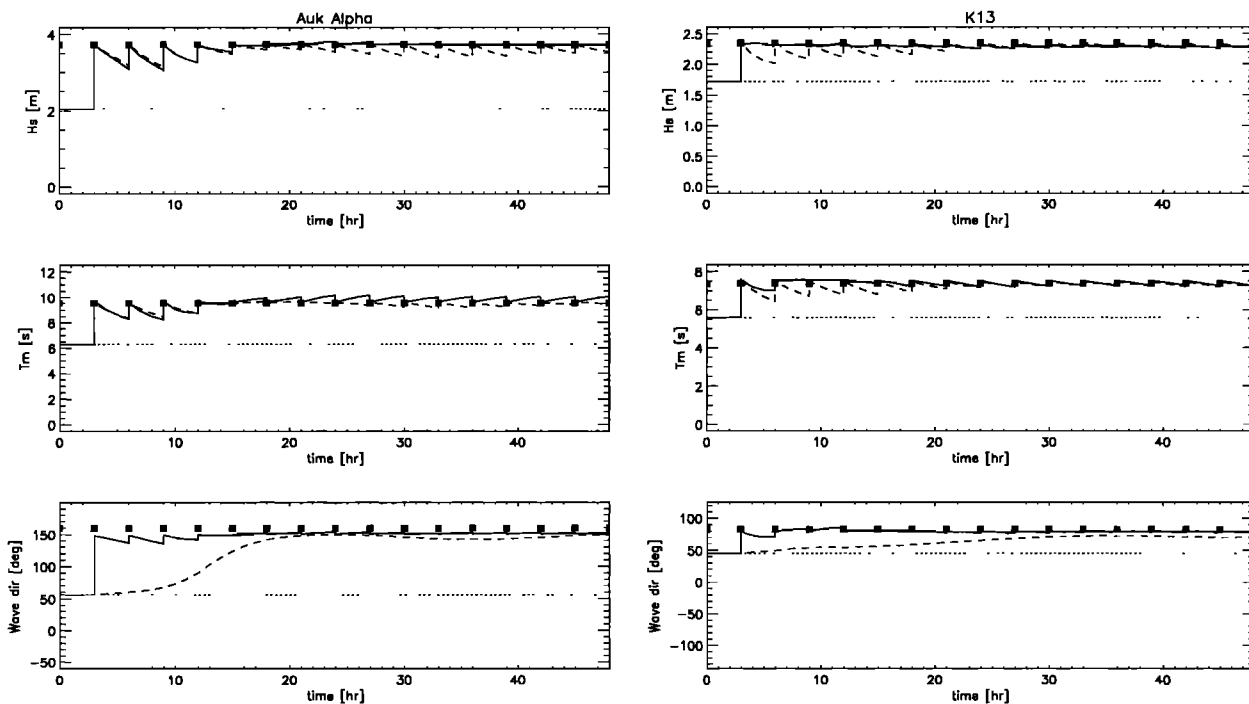


Figure 8. Time series of significant wave height, mean wave period, and mean direction for experiment S3: (left) Auk Alpha and (right) K13. Line types are as in Figure 6.

well, and the difference in performance between the two schemes is small in most cases. This is to be expected if one wave system dominates the spectrum, of which the mean direction is predicted well in the first guess. This is the case during most of the investigated period.

However, two interesting exceptions to this situation can be noted, especially at IJmuiden. From May 12 to 13, the mean wave direction of the NOASS run deviates from the observations by 20° to 30° (Figure 12, bottom right panel). This is corrected only by the OI-P assimilation scheme and not by the OI-I scheme, which is to be expected since the directional information is missing in the latter scheme. The second time that the schemes differ in performance is at the end of May 14 and the beginning of May 15. This is the moment when, at IJmuiden, the northerly swell is diminishing in strength and a new, southwesterly wind sea is growing (Figure 13). At first, this wind sea is missed entirely by the NOASS run, presumably because of an inaccurate modeling of the wind which is rapidly changing in the southern North Sea at that time. As can be seen from the top panels of Figure 13, the wind sea system is also missed initially by both assimilation schemes. For the OI-I scheme, this is to be expected. The OI-P run also misses the wind sea peak at first, because some energy of the new wave system should already be present in the model first-guess before a corresponding wave partition can be created (see subsection 5.6). A few hours later, when the wind sea system appears in the first guess, the spectral distribution and mean wave direction are quickly corrected by the OI-P scheme (Figure 12, bot-

tom right panel; Figure 13, bottom panels). In the OI-I run, on the other hand, the northerly swell remains overestimated and the wind sea remains underestimated for several more hours.

Figure 14 shows two 24-hour forecast time series after assimilation with the OI-P scheme. The impact of the assimilation on the forecast at Auk Alpha is short-lived, since it is the most northern assimilation location. At IJmuiden, however, the impact is large (at least 24 hours) in the second forecast, which is dominated by swell. Here optimal profit is made of the assimilation of the swell at the more northern locations. In the first, wind-sea-dominated forecast, the impact is much smaller.

In summary, both schemes correct the systematic underprediction of wave height by the model during the whole period. This improves the forecast typically over a period of 12 hours and longer when northerly swell dominates. In the periods when the wave direction is modeled inaccurately (May 12 and May 15), the OI-P scheme is clearly superior to the OI-I scheme.

8. Conclusions

A wave data assimilation scheme is presented which is based on the partitioning of the wave spectrum into separate wave systems and subsequent optimal interpolation of the mean parameters of these partitions. It is specifically designed to perform the partitioning on the incomplete spectral information which can be extracted from pitch-and-roll buoys. The scheme has been imple-

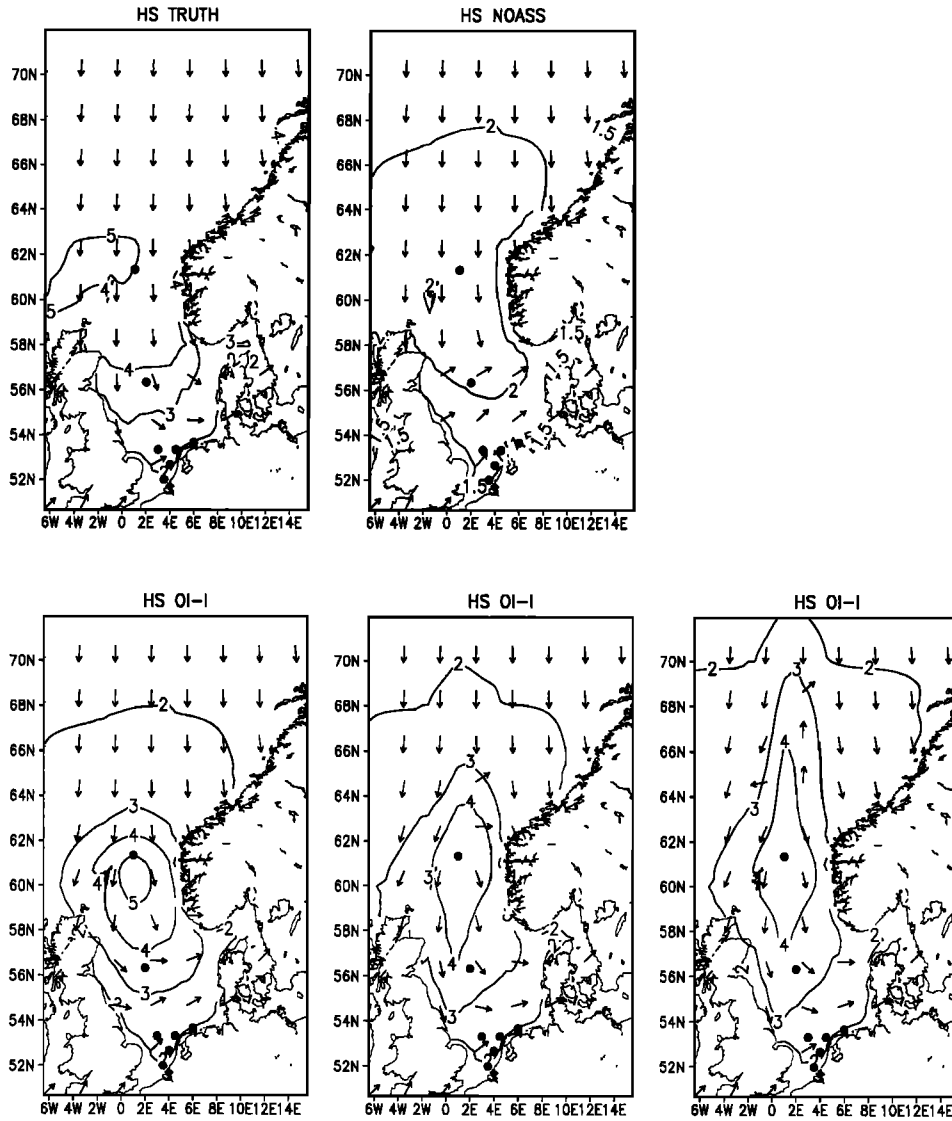


Figure 9. Significant wave height fields for experiment S3. The top row shows true and NOASS fields. The bottom row shows, from left to right, results of the OI-I scheme, after 4, 8, and 12 assimilation steps (12, 24, and 36 hours, respectively, after start of the assimilation run). Contours indicate wave height; arrows indicate mean wave direction.

mented in an operational North Sea wave model. It is very efficient: the analysis takes only a fraction of the computation time needed for a wave model run.

The scheme was tested and its performance has been compared to an assimilation scheme which only assimilates integrated wave parameters, in order to determine the effect of directional observations on the wave analysis and forecast. First it was tested in a few identical twin experiments and then in a hindcast with real wave and wind data.

First of all, we conclude that the assimilation experiments at the North Sea show an improvement both of the sea state analysis and of the forecast. The latter is not obvious, given the modest spatial dimensions of the North Sea. It is mostly due to timely detection and assimilation of swell coming from the Norwegian Sea,

which has a relatively long travel time to the southern North Sea. In favorable conditions, i.e., situations in which northerly swell is the dominant wave system in the North Sea, the positive impact of the assimilation can be seen up to around 24 hours in forecast.

We have demonstrated the advantage of assimilating spectral wave data from pitch-and-roll buoys over the assimilation of significant wave height and mean wave period only, which is the case in many operational assimilation schemes. Both in the artificial experiments and in the hindcast with real data, the partitioning scheme appeared to perform better in cases where the first-guess wave direction was wrong or where multiple wave systems were present at the same time.

Finally, the synthetic experiments show that both schemes tend to overcompensate for model-observation

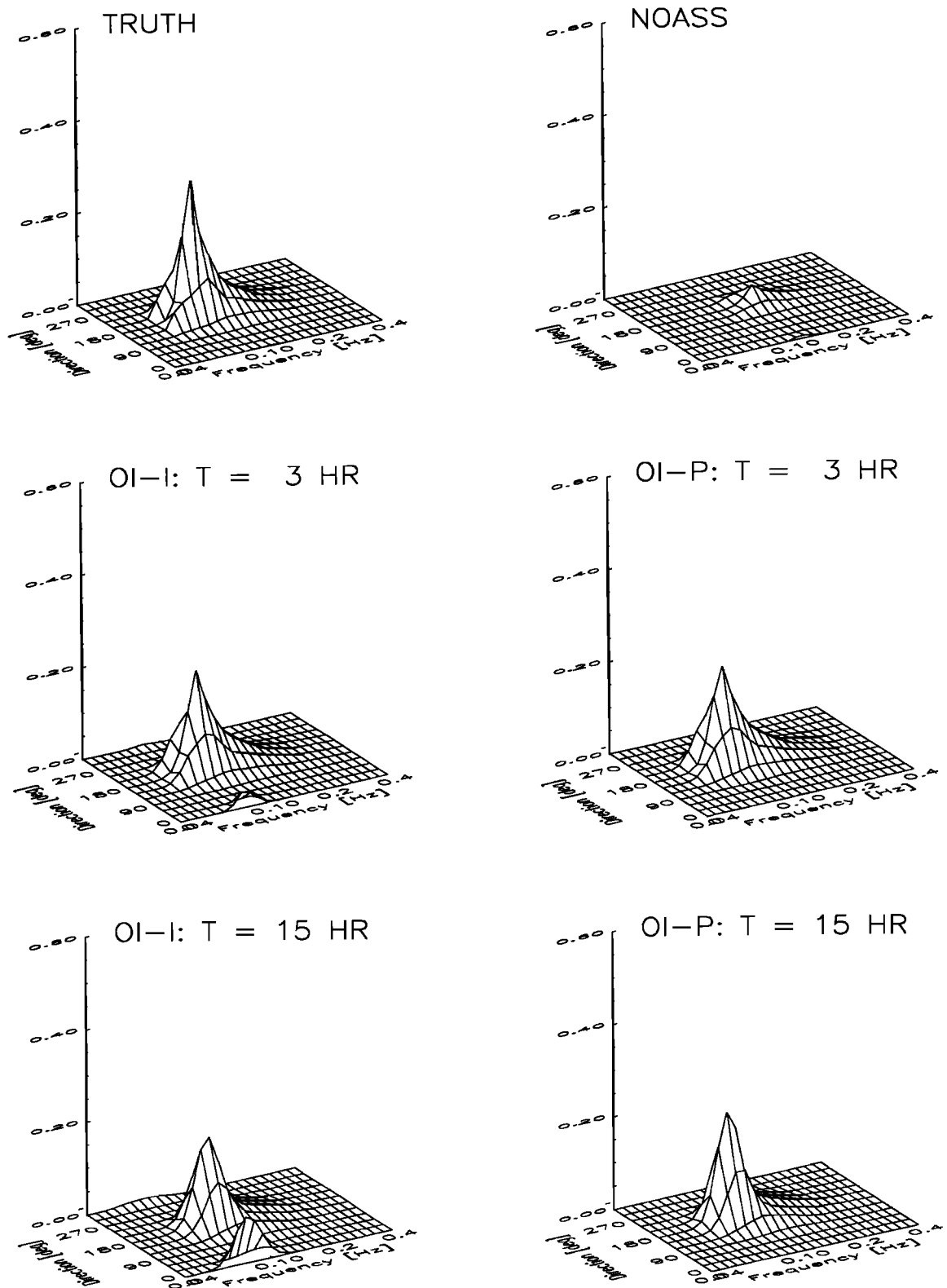


Figure 10. Wave spectra at North Cormorant for experiment S3 for the truth run (top left), the NOASS run (top right), and after the first (middle panels) and fifth (bottom panels) assimilation steps with the (left) OI-I scheme and (right) OI-P scheme.

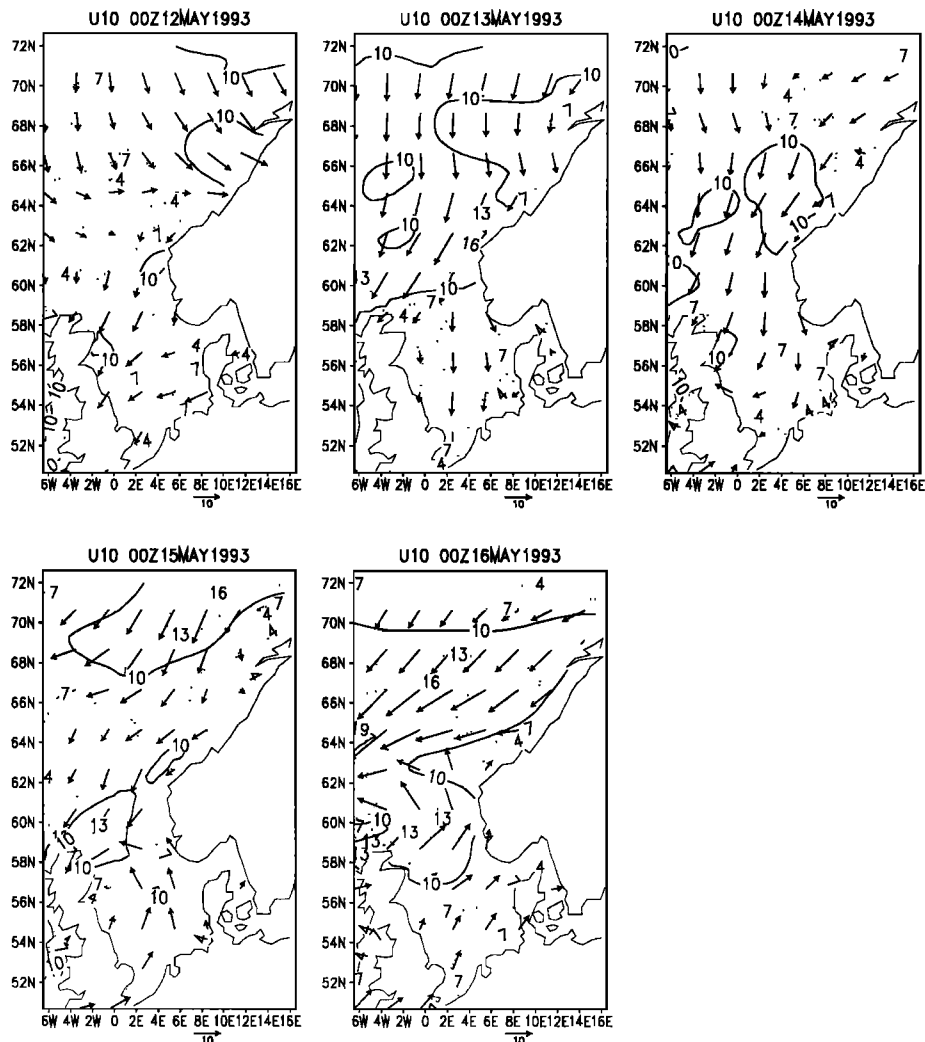


Figure 11. HIRLAM analyzed wind fields for the period May 12 to May 16, 1993.

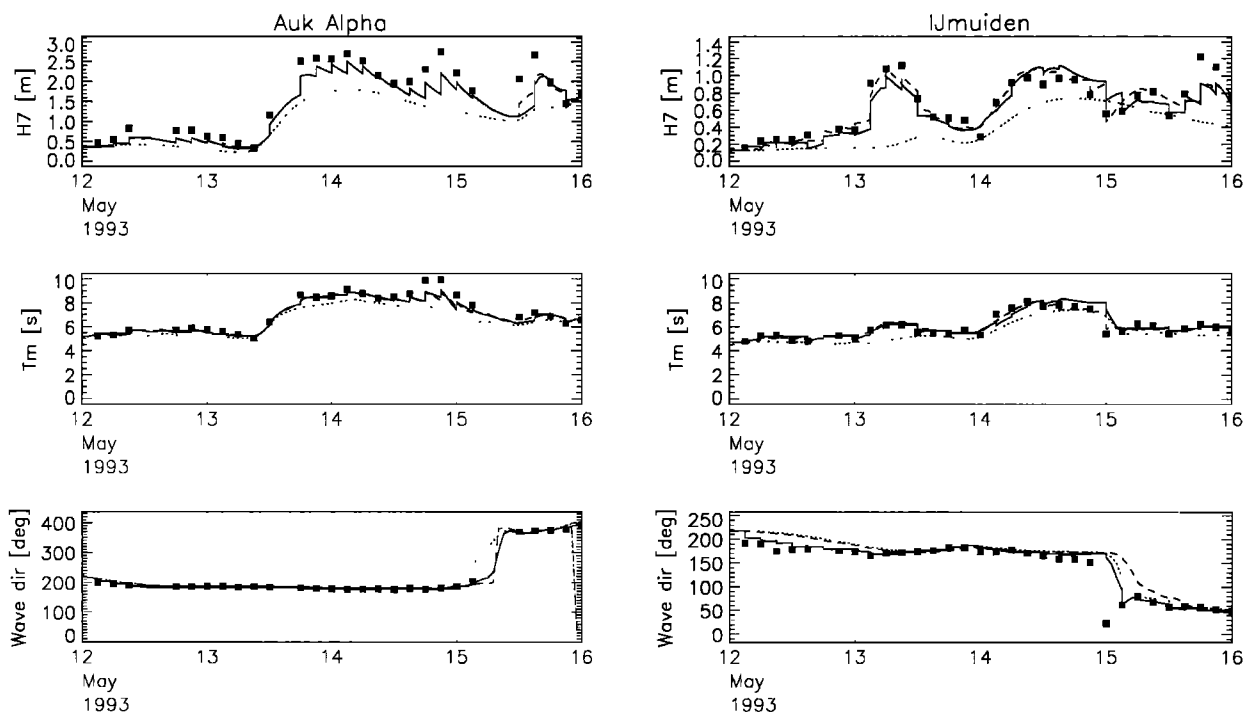


Figure 12. Time series of (top) low-frequency wave height, (middle) mean wave period and (bottom) mean direction for the May 1993 hindcast for (left) Auk Alpha and (right) IJmuiden. Line types are as in Figure 6.

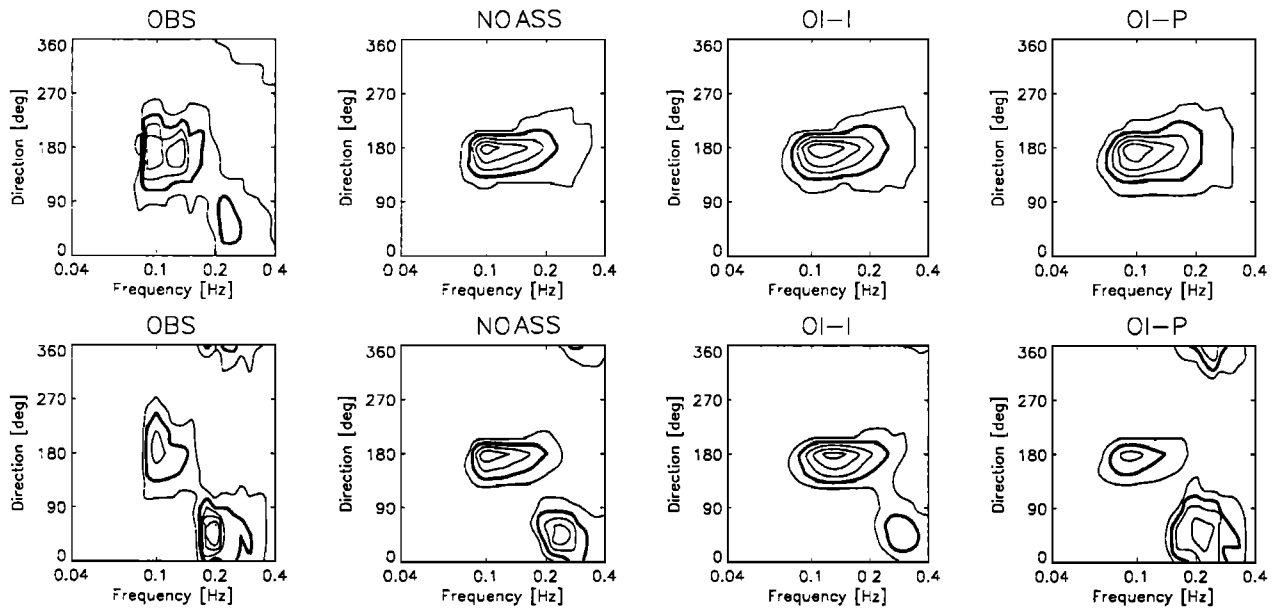


Figure 13. Spectra at IJmuiden (top) at May 14, 2100 UT and (bottom) at May 15, 0300 UT. From left to right are shown observation, NOASS run, OI-I analysis, and OI-P analysis.

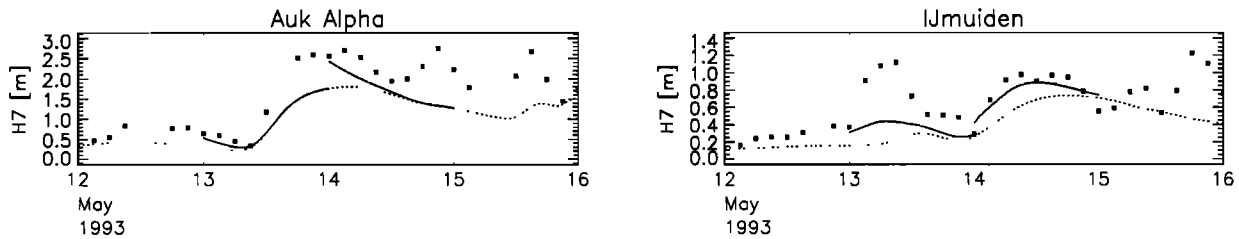


Figure 14. Two 24-hour forecasts after assimilation with the OI-P scheme, starting at May 13, 0000 UT, and May 14, 0000 UT, respectively (solid lines), for (left) Auk Alpha and (right) IJmuiden. Boxes, observations; dotted lines, NOASS run.

differences when conditions at sea are stable, because the gain in accuracy of the model state after assimilation is not taken into account. This can only be done properly by a dynamically consistent, i.e., time-dependent assimilation scheme.

In the near future, the present scheme will be tested further in an operational forecasting setting. Various improvements on the scheme are under investigation. Already some experience has been obtained with the introduction of more refined error covariance parameterizations (e.g., wave-direction-dependent correlation length). Better treatment of nonassigned partitions may prevent discarding valuable observations. Furthermore, it should be relatively straightforward to merge the OI-I and OI-P approaches in order to handle both spectral and integral observations (e.g., altimeter wave height measurements) simultaneously. Finally, research will concentrate on the incorporation of the model dynamics in the assimilation procedure.

Acknowledgments.

The authors would like to thank B. Roskam from Rijkswaterstaat, Netherlands, for supplying the wave buoy data, and J. Onvlee from KNMI for the supply and maintenance of the operational wave model. Valuable discussions with P. ten Brummelhuis (Delft Hydraulics) and G. Burgers and G. Komen (KNMI) are acknowledged. Part of this work was carried out in the framework of the European Coupled Atmosphere/Wave/Ocean (ECAWOM) project, which is funded by the MAST (Marine Science and Technology) Programme of the European Union. A.C. Voorrips was supported by the Technology Foundation (STW) and is partly affiliated with Delft University of Technology, Faculty of Technical Mathematics and Informatics, P.O. Box 5031, Delft, Netherlands.

References

- Barzel, G., and R.B. Long, Wave model fitting using the adjoint technique, in *Dynamics and modelling of ocean waves*, edited by G.J. Komen et al., pp. 447-453, Cambridge Univ. Press, New York, 1994.

- Bidlot, J.-R., F. Ovidio, and D. Van den Eynde, Validation and improvement of the quality of the operational wave model MU-WAVE by the use of ERS-1 satellite data, *Rep. MUMM/T3/AR04*, 53 pp., Management Unit of the Mathematical Model of the North Sea, Brussels, Belgium, 1995.
- Breivik, L.-A., and M. Reistad, Assimilation of ERS-1 altimeter wave heights in an operational numerical wave model, *Weather Forecasting*, *9*(3), 440-451, 1994.
- Brüning, C., and S. Hasselmann, Extraction of wave spectra from ERS-1 SAR wave mode spectra by an improved SAR inversion scheme, in *Proceedings First ERS-1 Pilot Project Workshop, Toledo, Spain, 22-24 June 1994*, *Eur. Space Agency Spec. Publ., ESA SP-365*, 45-48, 1994.
- Burgers, G., V.K. Makin, G. Quanduo, and M. de las Heras, Wave data assimilation for operational wave forecasting at the North Sea, paper presented at the 3rd International Workshop on Wave Hindcasting and Forecasting, Environment Canada, Montreal, Quebec, Canada, May 19-22, 1992.
- de las Heras, M.M., G. Burgers, and P.A.E.M. Janssen, Variational wave data assimilation in a third-generation wave model, *J. Atmos. Oceanic Technology*, *11*, 1350-1369, 1994.
- de las Heras, M.M., G. Burgers, and P.A.E.M. Janssen, Wave data assimilation in the WAM wave model, *J. Marine Syst.*, *6*, 77-85, 1995.
- de Valk, C.F., and C.J. Calkoen, Wave data assimilation in a third generation wave prediction model for the North Sea - An optimal control approach, *Rep. X38*, 123 pp., Delft Hydraul. Lab., Delft, Netherlands, 1989.
- Esteva, D.C., Evaluation of preliminary experiments assimilating Seasat significant wave heights into a spectral wave model, *J. Geophys. Res.*, *93*, 14,099-14,106, 1988.
- Gerling, T.W., Partitioning sequences and arrays of directional ocean wave spectra into component wave systems, *J. Atmos. Oceanic Technol.*, *9*, 444-458, 1992.
- Günther, H., S. Hasselmann, and P.A.E.M. Janssen, Wamod Cycle 4, *Tech. Rep. 4*, 102 pp., Deutsches Klimarechenzentrum, Hamburg, Germany, 1992.
- Günther, H., P. Lionello, and B. Hanssen, The impact of the ERS-1 altimeter on the wave analysis and forecast, *Rep. GKSS 93/E/44*, 56 pp., GKSS Forschungszentrum Geesthacht, Geesthacht, Germany, 1993.
- Hasselmann, S., C. Brüning, and P. Lionello, Towards a generalized optimal interpolation method for the assimilation of ERS-1 SAR retrieved wave spectra in a wave model, *Proceedings Second ERS-1 Symposium, Oct. 11-14, 1993, Hamburg, Germany*, *Eur. Space Agency Spec. Publ., ESA SP-361*, 21-25, 1994.
- Hasselmann, S., C. Brüning, K. Hasselmann, and P. Heimbach, An improved algorithm for the retrieval of ocean wave spectra from synthetic aperture radar image spectra, *J. Geophys. Res.*, *101*, 16,615-16,629, 1996.
- Janssen, P.A.E.M., P. Lionello, M. Reistad, and A. Hollingsworth, Hindcasts and data assimilation studies with the WAM model during the Seasat period, *J. Geophys. Res.*, *94*, 973-993, 1989.
- Källberg, P. (ed.), The HIRLAM forecast model, level 1, documentation manual, Swedish Meteorological and Hydrological Institute, Norrköping, Sweden, 1990.
- Komen, G.J., Introduction to wave models and assimilation of satellite data in wave models, in *The use of satellites in climate models*, *Eur. Space Agency Spec. Publ., ESA SP-221*, 21-25, 1985.
- Komen, G.J., Wave models, in *Report on the Workshop on Assimilation of Wind and Wave Data in Numerical Weather and Wave Prediction Models, ICSU-WMO-IOC-SCOR publ. WMO/TD 148-WCP-122*, pp. 26-28, World Meteorol. Org., Geneva, Switzerland, 1986.
- Komen, G.J., L. Cavaleri, M. Donelan, K. Hasselmann, S. Hasselmann, and P.A.E.M. Janssen, *Dynamics and Modelling of Ocean Waves*, Cambridge Univ. Press, New York, 1994.
- Kuik, A.J., G.P. van Vledder, and L.H. Holthuijsen, A method for the routine analysis of pitch-and-roll buoy wave data, *J. Phys. Oceanogr.*, *19*, 1020-1034, 1988.
- Lionello, P., and P.A.E.M. Janssen, Assimilation of altimeter measurements to update swell spectra in a wave model, paper presented at the International Symposium on Assimilation of Observations in Meteorology and Oceanography, World Meteorol. Org., Clermont-Ferrand, France, Aug. 1990.
- Lionello, P., H. Günther, and P.A.E.M. Janssen, Assimilation of altimeter data in a global third-generation wave model, *J. Geophys. Res.*, *97*, 14,453-14,474, 1992.
- Lionello, P., H. Günther, and B. Hanssen, A sequential assimilation scheme applied to global wave analysis and prediction, *J. Mar. Syst.*, *6*, 87-107, 1995.
- Long, R.B., and K. Hasselmann, A variational technique for extracting directional spectra from multicomponent wave data, *J. Phys. Oceanogr.*, *9*, 373-381, 1979.
- Longuet-Higgins, M.S., D.E. Cartwright, and N.D. Smith, Observations of the directional spectrum of sea waves using the motions of a floating buoy, in *Ocean Wave Spectra*, pp. 111-136, Prentice-Hall, Englewood Cliffs, N.J., 1963.
- Lygre, A., and H.E. Krogstad, Maximum entropy estimation of the directional distribution in ocean wave spectra, *J. Phys. Oceanogr.*, *16*, 2052-2060, 1986.
- Mastenbroek, C., V.K. Makin, A.C. Voorrips, and G.J. Komen, Validation of ERS-1 altimeter wave height measurements and assimilation in a North Sea wave model, *Global Atmos. Ocean Syst.*, *2*, 143-161, 1994.
- Monbaliu, J., Wind driven seas: Optimal parameter choice for the wind input term, *J. Wind Eng. and Ind. Aerodyn.*, *41-44*, 2499-2510, 1992.
- Thomas, J., Retrieval of energy spectra from measured data for assimilation into a wave model, *Q. J. R. Meteorol. Soc.*, *114*, 781-800, 1988.
- Tucker, M.J., *Waves in ocean engineering: measurement, analysis, interpretation*, 431 pp., Ellis Horwood, Chichester, England, 1991.
- Wave Model Development and Implementation (WAMDI) Group, The WAM model - A third generation ocean wave prediction model, *J. Phys. Oceanogr.*, *15*, 566-592, 1988.

S. Hasselmann, Max-Planck-Institut für Meteorologie, Bundesstraße 55, D-20146 Hamburg, Germany. (e-mail: susanne.hasselmann@dkrz.de)

A.C. Voorrips and V.K. Makin, Royal Netherlands Meteorological Institute, P.O. Box 201, 3730 AE De Bilt, Netherlands. (e-mail: voorrips@knmi.nl; makin@knmi.nl)

(Received February 6, 1996; revised September 17, 1996; accepted October 16, 1996.)